

H-COUP Version 3:
A program for one-loop corrected decays of any Higgs bosons
in non-minimal Higgs models

Masashi Aiko,^{1,*} Shinya Kanemura,^{2,†} Mariko Kikuchi,^{3,‡} Kodai Sakurai,^{4,5,§} and Kei Yagyu^{2,¶}

¹*KEK Theory Center, IPNS, KEK, Tsukuba, Ibaraki 305-0801, Japan*

²*Department of Physics, Osaka University, Toyonaka, Osaka 560-0043, Japan*

³*College of Engineering, Nihon University, Koriyama, Fukushima 963-8642, Japan*

⁴*Institute of Theoretical Physics, Faculty of Physics,*

University of Warsaw, ul. Pasteura 5, PL-02-093 Warsaw, Poland

⁵*Department of Physics, Tohoku University, Sendai, Miyagi 980-8578, Japan*

The H-COUP program is provided as a package of Fortran codes, which can compute observables related to Higgs bosons including radiative corrections in various extended Higgs sectors. We give a manual for the latest version of H-COUP (H-COUP_3.0), in which decay rates and branching ratios of all the Higgs bosons can be calculated at one-loop level in EW and Higgs interactions with QCD corrections in the Higgs singlet model, four types of the two Higgs doublet model with a softly-broken Z_2 symmetry, and the inert doublet model. The previous version (H-COUP_2.0) can evaluate those only for the standard model like Higgs boson with the mass of 125 GeV (h). In H-COUP_3.0, renormalized quantities are computed based on the gauge independent on-shell renormalization scheme. The source code of H-COUP_3.0 can be downloaded via the following link: <http://www-het.phys.sci.osaka-u.ac.jp/~hcoup>. By using H-COUP_3.0, we can compare the precise measurements of the properties of h and direct searches for additional Higgs bosons with their predictions at one-loop level, by which we can reconstruct the structure of the Higgs sector.

* maiko@post.kek.jp

† kanemu@het.phys.sci.osaka-u.ac.jp

‡ kikuchi.mariko13@nihon-u.ac.jp

§ kodai.sakurai.e3@tohoku.ac.jp

¶ yagyu@het.phys.sci.osaka-u.ac.jp

I. INTRODUCTION

The LHC experiments have clarified the existence of the 125 GeV Higgs boson and its properties to be consistent with those of the Higgs boson in the Standard Model (SM) within the theoretical and experimental uncertainties [1, 2]. However, the nature of electroweak symmetry breaking is still one of the most important questions in particle physics. In fact, no fundamental principle has been proved for determining the structure of the Higgs sector. Indeed, the SM merely assumes the minimal form composed of an isospin scalar doublet field. Thus, there is no compelling reason to stay at the minimal form, and are various possibilities for extended structures of the Higgs sector. On the other hand, the SM obviously cannot explain tiny neutrino masses, existence of dark matter and baryon asymmetry of the Universe, so that new physics must exist. The question is then what is the scale of new physics, which could be much higher than the electroweak scale, e.g., in the conventional seesaw scenario or could be EW/TeV scales, e.g., in the electroweak baryogenesis. If the latter is realized, its experimental verification is expected. In particular, it is quite natural to think that the Higgs sector is modified from the minimal form. In fact, extended Higgs sectors are often introduced in new physics at TeV scale, e.g., models with an extra isospin singlet, doublet and triplet field and so on, and their property strongly depends on new physics scenario. Therefore, unveiling the true structure of the Higgs sector is a key to open the door to new physics.

The structure of the Higgs sector can be determined by investigating various extended Higgs sectors comprehensively. There are basically two ways for such an investigation, i.e., precise measurements for properties of the discovered Higgs boson (h) and direct searches for extra Higgs bosons.

The former is absolutely important, because the precise measurement of h is what we can definitely perform at future collider experiments such as the High-Luminosity LHC (HL-LHC) [3] and lepton colliders, e.g., the International Linear Collider (ILC) [4–7], the Circular Electron-Positron Collider (CEPC) [8] and e^+e^- collisions of the Future Circular Collider (FCC-ee) [9]. For example, the Higgs boson couplings are expected to be measured typically with a few percent level at HL-LHC [10] and a few permille level at e^+e^- colliders [10]. Thus, predictions of the Higgs boson couplings, decay rates and branching ratios in extended Higgs sectors must be evaluated at quantum levels in order to compare such precise measurements. Once deviations in the observables of h from SM predictions are found, we can extract the scale of new physics from the size of deviations, which has been known as a “new no-loose theorem” [11]. Moreover, we can fingerprint the Higgs sector, i.e., extracting the properties such as the representation and the number of Higgs

fields by measuring the pattern of deviations.

Detections of additional Higgs bosons are direct evidence of an extended Higgs sector. Although any clear signatures have not been observed yet, there are still possibilities of the existence of extra Higgs bosons at the electroweak scale, which is well motivated by various new physics scenarios, e.g., the radiative seesaw mechanism, the Higgs-portal dark matter and the electroweak baryogenesis. It has been known that the decay property of extra Higgs boson strongly depends on the “alignmentness” of the Higgs sector, i.e., how the property of h is close to the one in the SM Higgs boson. In the nearly alignment case, extra Higgs bosons tend to dominantly decay into a bosonic final state, e.g., $H \rightarrow W^+W^-/ZZ/hh$, $A \rightarrow Zh$ and $H^\pm \rightarrow W^\pm h$ in the Two Higgs Doublet Models (THDMs), in which severe lower limits on the mass of extra Higgs bosons have already been taken at the LHC [12–14]. This also means that a lower limit and an upper limit on the mass of extra Higgs bosons can simultaneously be taken by the synergy between the direct searches at the HL-LHC and the precise measurements of h , and thus a large portion of the parameter space can be explored [12]. The important thing here is that loop effects of extra Higgs bosons can change the alignmentness and the decay rates of extra Higgs bosons at the same time. In particular, such modifications can be significant when non-decoupling effects of extra Higgs bosons are realized, which can appear in new physics scenarios, e.g., with first order electroweak phase transitions [15–17]. Therefore, including the effect of radiative corrections is important not only for the precise measurement of h , but also for the direct searches for extra Higgs bosons.

In order to realize the fingerprinting, to establish the new no-loose theorem and to perform the direct searches in a more precise way, we have developed the H-COUP program which is provided as a package of Fortran codes to evaluate Higgs boson related observables including radiative corrections in various extended Higgs sectors. So far, we have published the H-COUP version 1 (H-COUP_1) [18] and version 2 (H-COUP_2) [19], which can provide one-loop corrected couplings, decay rates and branching ratios of h in the THDMs with a softly-broken Z_2 symmetry to avoid flavor changing neutral currents at tree level, the Higgs Singlet Model (HSM) and the Inert Doublet Model (IDM) based on the gauge independent on-shell renormalization scheme [20].

In this paper, we extend the H-COUP program to version 3 (H-COUP_3.0) and give its manual, where the decay rates and the branching ratios of *all* the Higgs bosons can be evaluated at one-loop level in the extended Higgs sectors shown above. We have implemented one-loop corrected decay rates of extra Higgs bosons in H-COUP_3.0, which have been computed in the series of our papers [21–23]. In H-COUP_3.0, we take the same on-shell scheme for the scalar two-point functions as the previous versions, while the renormalization for the tadpole is performed by either the standard

tadpole scheme [24, 25] or the alternative tadpole scheme [26] (in the case of the THDMs, there are four choices because of the renormalization method of the other parameter). The users can choose these renormalization schemes. There are also important works relevant to such radiative corrections in the THDMs [27–34] and in the minimal supersymmetric SM [35–40].

We note that similar program tools have been developed by the different groups, e.g., `2HDECAY` [41], `Prophecy4f` [42], `ewN2HDECAY` [43] and `EWshDECAY` [44]¹. A remarkable feature of `H-COUP` is that it can systematically compute both the properties of h and extra Higgs bosons in various extended Higgs sectors under a fixed renormalization scheme.

This paper is organized as follows. In Sec. II, we briefly review the extended Higgs models which are implemented in `H-COUP_3.0` to define the notation. In Sec. III, we discuss the renormalized vertex functions and decay rates. We also explain our renormalization scheme. We then describe the structure of `H-COUP_3.0` and how to install and run the program in Sec. IV. In Sec. V, we show examples of the numerical evaluation. Summary is given in Sec. VI.

II. MODELS AND CONSTRAINTS

We define three models with the extended Higgs sector, i.e, the HSM, the THDMs and the IDM which are implemented in `H-COUP_3.0`. In Table I, we show the mass eigenstates of scalar fields, the input parameters and the constraints in each model. In the following, we provide additional explanations of Table I in each model, see the references given in this table for more details of the model description.

Throughout the paper, we denote the mass eigenstates of scalar fields as:

$$\begin{aligned}
 h &: \text{the discovered CP-even Higgs boson with the mass 125 GeV,} \\
 H &: \text{another CP-even Higgs boson,} \\
 A &: \text{a CP-odd Higgs boson,} \\
 H^\pm &: \text{a pair of singly charged Higgs bosons.}
 \end{aligned}
 \tag{1}$$

In the HSM, the Higgs sector is composed of the SM Higgs field Φ , i.e., the isospin doublet Higgs field with hypercharge $Y = 1/2$, and an isospin singlet scalar field S with $Y = 0$. In this model, no additional symmetry beyond the SM is imposed [52]. There are two mass eigenstates and five free input parameters as shown in Table I, where m_ϕ indicates a mass of a scalar boson

¹ Recently, `FlexibleDecay` [45] appeared, in which decays of Higgs bosons can be computed in the $\overline{\text{MS}}$ scheme with higher order electroweak and QCD corrections in various models beyond the SM.

Models	Mass eigenstates	Input parameters	References for constraints				
			(a), (b)	(c)	(d)	(e)	(f)
HSM [46, 47]	h, H	$m_H, \alpha, \lambda_S, \lambda_{\Phi S}, \mu_S$	[48–50]	[51]	[47, 52]	[47, 53]	[54]
THDMs [17, 55, 56] (Type-I, II, X, Y)	h, H, A, H^\pm	$m_H, m_A, m_{H^\pm}, M^2,$ $\sin(\beta - \alpha), \tan \beta$	[57–61]	[62–65]	[66]	[67]	[68–72]
IDM [73]	h, H, A, H^\pm	$m_H, m_A, m_{H^\pm}, \mu_2^2, \lambda_2$	[57–61]	[62–65]	[74]	[75]	[68–72]

TABLE I. Mass eigenstates of scalar fields, input free parameters and references in the HSM, the THDMs and the IDM. Although only free parameters beyond the SM are given, there are two SM parameters in the Higgs potential; i.e. the mass of the discovered Higgs boson ($m_h \simeq 125$ GeV) and the vacuum expectation value (VEV) ($v \simeq 246$ GeV), in each model. The numbers in “References of constraints” indicate kinds of constraints as; (a) Vacuum stability at tree level, (b) Vacuum stability (RGE improved), (c) Tree-level unitarity, (d) True vacuum, (e) Triviality, (f) Electroweak S and T parameters.

ϕ , and α is the mixing angle between two CP-even Higgs bosons with its domain to be defined as $-\pi/2 \leq \alpha \leq \pi/2$. The other three parameters $\lambda_S, \lambda_{\Phi S}$ and μ_S are the coefficients of the $S^4, |\Phi|^2 S^2$ and S^3 terms in the Higgs potential, respectively.

The THDMs contain two isospin doublet Higgs fields Φ_1 and Φ_2 with $Y = 1/2$. In H-COUP, we impose a softly-broken Z_2 symmetry [76] to avoid flavor changing neutral currents at tree level, in which Φ_1 and Φ_2 are assigned to be Z_2 -even and Z_2 -odd, respectively. Depending on the charge assignments of right-handed fermions, four types of Yukawa interactions appear, which are so-called Type-I, Type-II, Type-X and Type-Y [77–80]. There are five mass eigenstates and six input parameters described in Table I, where α is the mixing angles between two CP-even Higgs bosons and $\tan \beta$ is the ratio of the VEVs $\tan \beta = v_2/v_1$ ². We define $\sin(\beta - \alpha) \geq 0$ and $\tan \beta > 0$. A dimensionful parameter M^2 describes the soft breaking scale of the Z_2 symmetry.

In the IDM, the Higgs sector also consists of two isospin doublet Higgs fields Φ and η with $Y = 1/2$, so that five mass eigenstates appear as those in the THDMs. Unlike the THDMs, an unbroken Z_2 symmetry [57, 81] is imposed instead of the softly-broken one, in which only η is assigned to be Z_2 -odd and all the other fields are assigned to be Z_2 -even. Thanks to the unbroken Z_2 symmetry, the lightest additional neutral scalar boson (H or A) can be a candidate for dark matter. There are five free parameters shown in Table I, where λ_2 and μ_2^2 are the coefficients of the quartic and the quadratic terms of η , respectively.

² In addition, we have to input the sign of $\cos(\beta - \alpha)$ because values of α and β are not directly input.

In each model, the following constraints can be imposed in H-COUP_3.0 as in the previous versions:

- (a) Vacuum stability at tree level [57]
- (b) Vacuum stability (Renormalization group equations (RGE) improved with the cutoff)
- (c) Tree-level unitarity [82]
- (d) True vacuum [66, 83]
- (e) Triviality (with the cutoff scale) [67].
- (f) Electroweak S and T parameters [84, 85]

In Table I, we list the references for these constraints in each model, see also the manual of H-COUP_1.0 [18] for details.

III. RENORMALIZED VERTICES AND DECAY RATES

In this section, we discuss radiative corrections to the decay rate of a scalar boson ϕ after introducing renormalization schemes implemented in H-COUP_3.0. While the discussions of the renormalization schemes are model-dependent, the formulation of the decay rate is carried out in a model-independent way.

A. Renormalization schemes

The renormalization of Higgs potential parameters is performed by making use of on-shell conditions for two-point functions of the scalar states. With the on-shell conditions, masses, mixing angles, and wave functions renormalization factors for the scalar states are defined as on-shell parameters. In Ref. [86], it has been pointed out that the on-shell renormalization of scalar mixing angles give rise to gauge-dependent amplitudes. In order to remove such gauge dependence, we make use of the pinch technique [87], in which appropriate pinch terms are added for the counterterms of the mixing angles.

The UV divergence of the one-point functions of Higgs fields should also be taken away in the renormalized Higgs potential. For the renormalization of tadpoles, there are two different

Models	On-shell renormalization	$\overline{\text{MS}}$ renormalization	Refs.
HSM	$\delta m_h^2, \delta m_H^2, \delta\alpha, \delta Z_\phi, \delta C_\phi$	$\delta\lambda_{\Phi S}, \delta\mu_S$	[47]
THDMs	$\delta m_h^2, \delta m_H^2, \delta m_A^2, \delta m_{H^\pm}^2, \delta\alpha, \delta\beta, \delta Z_\phi, \delta C_\phi$	δM^2 (or δm_{12}^2)	[56]
IDM	$\delta m_h^2, \delta m_H^2, \delta m_A^2, \delta m_{H^\pm}^2, \delta Z_\phi$	$\delta\mu_2^2$	[73]

TABLE II. Counterterms used in the computations of decays of scalar bosons in the HSM, the THDMs, and the IDM. In the wave function factors δZ_ϕ and δC_ϕ , the subscript “ ϕ ” denotes any of Higgs bosons listed in Table. I for each model. If one chooses the standard tadpole scheme, the counterterms for tadpoles should be also added. Detailed discussions about the renormalization of these counterterms can be found in the quoted references. The gauge invariant renormalization of the mixing angles α and β can be found in Ref. [20].

renormalization schemes, which are called the standard tadpole scheme [24, 25] and the alternative tadpole scheme [26] (also see a new scheme for tadpole renormalization in recent works [88, 89]). Let us briefly describe how the renormalization of tadpoles is performed in these two schemes. In the standard tadpole scheme, *renormalized* tadpoles are set to zero. One then has the tadpole counterterms, which eliminate the UV divergence for the one-point functions by renormalization conditions for tadpoles, i.e., $\hat{\Gamma}_h = \Gamma_h^{\text{1PI}} + \delta T_h = 0$ for the SM-like Higgs boson h . In contrast, in the alternative tadpole scheme, *unrenormalized* tadpoles are set to zero, which means that the tadpole counterterm parameters are not introduced in a theory. Instead, there is a degree of freedom to shift bare Higgs fields, $\phi_B \rightarrow \phi_B + \Delta v$. This shift introduces an additional tadpole term, and one can choose the constant Δv in a way that the tadpole terms vanish at loop level, i.e., $\Gamma_h^{\text{1PI}} + m_h^2 \Delta v = 0$ for the SM-like Higgs boson h . The shift affects all terms containing the Higgs bare field ϕ_B . Because of this, one eventually should include tadpole-inserted diagrams in renormalized self-energies and renormalized vertex functions.

In all the models implemented in H-COUP_3.0, the number of input parameters is greater than that determined by the on-shell conditions for the scalar two-point functions. Thus, the other remaining parameters should be renormalized in different ways. As briefly discussed, such a parameter is determined by the $\overline{\text{MS}}$ renormalization. In the following, by specifying a model, we discuss how each input parameter is renormalized and introduce renormalization schemes implemented in H-COUP_3.0. The renormalization of model parameters is summarized in Table II.

Higgs singlet model

In the HSM, there are two mass parameters (i.e., m_h and m_H), one mixing angle and four

parameters of wave function renormalizations. They are renormalized by on-shell conditions for two-point functions of h and H , and the other parameters $\lambda_{\Phi S}$ and μ_S are determined by the $\overline{\text{MS}}$ renormalization. Since there are two different ways to renormalize tadpoles as discussed above, in H-COUP_3.0, a user can choose the following renormalization schemes for the tadpoles in the HSM:

[KOSY]: Standard tadpole scheme

[PT]: Alternative tadpole scheme

The KOSY and the PT scheme schemes are respectively based on Ref. [17] and Ref. [20]. We here emphasize that the difference between these two renormalization schemes is how the tadpoles are renormalized. For all the above schemes, the scalar mixing angle α is commonly renormalized by the on-shell scheme with the pinch terms.

Two Higgs doublet models

In the THDMs, four mass parameters, two mixing angles, and twelve wave functions are determined by the on-shell renormalization. The remaining parameter M^2 is determined by the $\overline{\text{MS}}$ renormalization. This parameter is related to the softly-broken parameter of the Z_2 symmetry m_{12}^2 ($V \supset (m_{12}^2 \Phi_1^\dagger \Phi_2 + \text{h.c.})$) by $M^2 = m_{12}^2 / (\cos \beta \sin \beta)$. Instead of M^2 , one can also renormalize m_{12}^2 as a $\overline{\text{MS}}$ parameter. In H-COUP_3.0, a user can choose the renormalization scheme for the tadpoles and the $\overline{\text{MS}}$ parameter in the THDMs. Hence, the following four different renormalization schemes are implemented:

[KOSY1]: Standard tadpole scheme, δM^2

[PT1]: Alternative tadpole scheme, δM^2

[KOSY2]: Standard tadpole scheme, δm_{12}^2

[PT2]: Alternative tadpole scheme, δm_{12}^2

The KOSY1 and KOSY2 schemes are based on Ref. [17], while the PT1 and PT2 schemes are based on Ref. [20]. In all these renormalization schemes, the pinch technique is applied to the renormalization of the mixing angles α and β .

Inert doublet model

In the IDM, four mass parameters and four wave functions are determined by the on-shell renormalization. The invariant mass parameter μ_2^2 for the inert scalars is renormalized as a $\overline{\text{MS}}$ parameter. In Ref. [20], it has been shown that for renormalized vertex functions of h , the scheme difference between the standard tadpole scheme and the alternative tadpole scheme does not appear

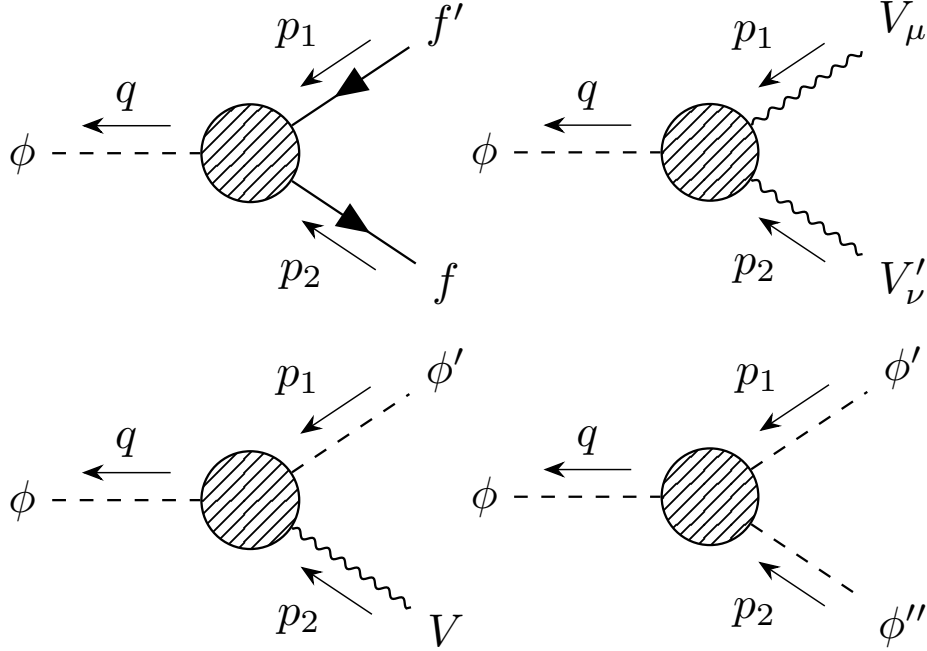


FIG. 1. Momentum assignment for the renormalized $\phi f f'$, $\phi V V'$, $\phi V \phi'$, and $\phi \phi' \phi''$ vertices.

in the SM. This is also the case in the IDM, because the counterterms for the renormalized vertex functions are expressed in the same form as those in the SM. Hence, for the IDM, we only implement the KOSY scheme based on Ref. [73] in H-COUP_3.0.

B. Renormalized vertex functions

When we consider two body final states, ϕ can generally decay into a fermion and an anti-fermion ($\phi \rightarrow f \bar{f}'$), two gauge bosons ($\phi \rightarrow V V'$), a gauge and a scalar bosons ($\phi \rightarrow V \phi'$) and two scalar bosons ($\phi \rightarrow \phi' \phi''$). In order to discuss radiative corrections to the decay rate of these modes, it is convenient to introduce the following renormalized vertices $\hat{\Gamma}_{\phi f f'}$, $\hat{\Gamma}_{\phi V V'}^{\mu\nu}$, $\hat{\Gamma}_{\phi V \phi'}^{\mu}$ and $\hat{\Gamma}_{\phi \phi' \phi''}$. Except for $\hat{\Gamma}_{\phi \phi' \phi''}$, each renormalized vertex can be decomposed into the following form factors:

$$\begin{aligned} \hat{\Gamma}_{\phi f f'}(p_1^2, p_2^2, q^2) &= \hat{\Gamma}_{\phi f f'}^S + \gamma_5 \hat{\Gamma}_{\phi f f'}^P + \not{p}_1 \hat{\Gamma}_{\phi f f'}^{V_1} + \not{p}_2 \hat{\Gamma}_{\phi f f'}^{V_2} \\ &\quad + \not{p}_1 \gamma_5 \hat{\Gamma}_{\phi f f'}^{A_1} + \not{p}_2 \gamma_5 \hat{\Gamma}_{\phi f f'}^{A_2} + \not{p}_1 \not{p}_2 \hat{\Gamma}_{\phi f f'}^T + \not{p}_1 \not{p}_2 \gamma_5 \hat{\Gamma}_{\phi f f'}^{\text{PT}}, \end{aligned} \quad (2)$$

$$\hat{\Gamma}_{\phi V V'}^{\mu\nu}(p_1^2, p_2^2, q^2) = g^{\mu\nu} \hat{\Gamma}_{\phi V V'}^1 + \frac{p_1^\nu p_2^\mu}{q^2} \hat{\Gamma}_{\phi V V'}^2 + i \epsilon^{\mu\nu\rho\sigma} \frac{p_{1\rho} p_{2\sigma}}{q^2} \hat{\Gamma}_{\phi V V'}^3, \quad (3)$$

$$\hat{\Gamma}_{\phi V \phi'}^{\mu}(p_1^2, p_2^2, q^2) = (p_1 + q)^\mu \hat{\Gamma}_{\phi V \phi'}, \quad (4)$$

where p_1^μ and p_2^μ denote the incoming momenta, and q^μ represents the outgoing momentum of ϕ , see Fig. 1. Each renormalized form factor $\hat{\Gamma}_{\phi XY}$ can be further divided into the following terms:

$$\hat{\Gamma}_{\phi XY}^i(p_1^2, p_2^2, q^2) = \Gamma_{\phi XY}^{i, \text{tree}} + \Gamma_{\phi XY}^{i, \text{loop}} \quad \text{with} \quad \Gamma_{\phi XY}^{i, \text{loop}} = \Gamma_{\phi XY}^{i, \text{1PI}} + \delta\Gamma_{\phi XY}^i, \quad (5)$$

where $\Gamma_{\phi XY}^{i, \text{tree}}$, $\Gamma_{\phi XY}^{i, \text{1PI}}$ and $\delta\Gamma_{\phi XY}^i$ respectively denote contributions from tree diagrams, 1PI diagrams and counterterms.

Let us also describe differences that can appear by using the different renormalization schemes in the HSM and the THDMs in order. In the HSM, the scheme difference between the KOSY scheme and the PT scheme only appears in $\hat{\Gamma}_{\phi\phi'\phi''}$ as can be seen in Ref. [20]. The analytical expressions can be found in the reference. The scheme difference does not appear in the other vertices $\hat{\Gamma}_{\phi ff'}$, $\hat{\Gamma}_{\phi V V'}^{\mu\nu}$ and $\hat{\Gamma}_{\phi V \phi'}^\mu$. In the THDMs, similar to the HSM, the scheme difference between the KOSY1 scheme and the PT1 scheme only arises for the renormalized vertex functions $\Gamma_{\phi\phi'\phi''}$. The scheme difference $\Delta\Gamma_{\phi\phi'\phi''}$ consists of the tadpole contributions, as given in Eqs.(A8), (A10) and (A12). On the other hand, no scheme difference appears for $\Gamma_{\phi\phi'\phi''}$ between the KOSY2 scheme and the PT2 scheme, so that these two schemes give the same results for all the decay processes of ϕ . In the end, three different results are obtained only for $\phi \rightarrow \phi'\phi''$ depending on these renormalization schemes in the THDMs. In Appendix. A, we present the analytical expressions for the scheme difference.

C. Radiative corrections to the decay rate

For decay processes that appear at the tree level, decay rates at NLO are generally expressed as

$$\begin{aligned} \Gamma(\phi \rightarrow XY)_{\text{NLO}} &= \Gamma(\phi \rightarrow XY)_{\text{LO}} [1 + \Delta_{\text{EW}}(\phi \rightarrow XY) - \Delta r + \Delta_{\text{QCD}}(\phi \rightarrow XY)] \\ &+ \Gamma(\phi \rightarrow XY\gamma), \end{aligned} \quad (6)$$

where $\Gamma(\phi \rightarrow XY)_{\text{LO}}$ is the decay rate at LO, $\Delta_{\text{EW}}(\phi \rightarrow XY)$ is the electroweak correction, $\Delta_{\text{QCD}}(\phi \rightarrow XY)$ is the QCD correction and $\Gamma(\phi \rightarrow XY\gamma)$ is the contribution from the real photon emission which is required to guarantee IR divergence-free results. The contribution from the real photon emission vanishes when ϕ , X , and Y are electrically neutral. We separately show the contribution from the electroweak correction to the muon decay, Δr , which appears by the

replacement of the VEV, i.e., $v^2 \rightarrow v^2(1 + \Delta r)$. The decay rates at LO are expressed as

$$\Gamma(\phi \rightarrow f\bar{f}')_{\text{LO}} = N_c^f \frac{m_\phi}{8\pi} \lambda^{1/2}(x_f, x_{f'}) \times \left[(|\Gamma_{\phi f f'}^{\text{S,tree}}|^2 + |\Gamma_{\phi f f'}^{\text{P,tree}}|^2)(1 - x_f - x_{f'}) - 2(|\Gamma_{\phi f f'}^{\text{S,tree}}|^2 - |\Gamma_{\phi f f'}^{\text{P,tree}}|^2)\sqrt{x_f x_{f'}} \right], \quad (7)$$

$$\Gamma(\phi \rightarrow VV')_{\text{LO}} = \frac{|\Gamma_{\phi V V'}^{\text{1,tree}}|^2}{64\pi m_\phi(1 + \delta_{VV'})} \frac{\lambda(x_V, x_{V'}) + 12x_V x_{V'}}{x_V x_{V'}} \lambda^{1/2}(x_V, x_{V'}), \quad (8)$$

$$\Gamma(\phi \rightarrow V\phi')_{\text{LO}} = \frac{|\Gamma_{\phi V \phi'}^{\text{tree}}|^2}{16\pi} \frac{m_\phi^3}{m_V^2} \lambda^{3/2}(x_V, x_{\phi'}), \quad (9)$$

$$\Gamma(\phi \rightarrow \phi'\phi'')_{\text{LO}} = \frac{|\Gamma_{\phi \phi' \phi''}^{\text{tree}}|^2}{16\pi m_\phi(1 + \delta_{\phi' \phi''})} \lambda^{1/2}(x_{\phi'}, x_{\phi''}), \quad (10)$$

where $N_c^f = 3$ (1) for f to be quarks (leptons), $x_a = m_a^2/m_\phi^2$ and $\lambda(x, y) = (1 - x - y)^2 - 4xy$. In the above expressions, V and V' are either W^\pm or Z ³. The electroweak corrections Δ_{EW} are expressed for each process as

$$\Delta_{\text{EW}}(\phi \rightarrow f\bar{f}') = \left[(|\Gamma_{\phi f f'}^{\text{S,tree}}|^2 + |\Gamma_{\phi f f'}^{\text{P,tree}}|^2)(1 - x_f - x_{f'}) - 2(|\Gamma_{\phi f f'}^{\text{S,tree}}|^2 - |\Gamma_{\phi f f'}^{\text{P,tree}}|^2)\sqrt{x_f x_{f'}} \right]^{-1} \times \left[2 \left\{ \text{Re}[\Gamma_{\phi f f'}^{\text{S,tree}} \Gamma_{\phi f f'}^{\text{loop}*}] + \text{Re}[\Gamma_{\phi f f'}^{\text{P,tree}} \tilde{\Gamma}_{\phi f f'}^{\text{loop}*}] \right\} (1 - x_f - x_{f'}) - 4 \left\{ \text{Re}[\Gamma_{\phi f f'}^{\text{S,tree}} \Gamma_{\phi f f'}^{\text{loop}*}] - \text{Re}[\Gamma_{\phi f f'}^{\text{P,tree}} \tilde{\Gamma}_{\phi f f'}^{\text{loop}*}] \right\} \sqrt{x_f x_{f'}} \right] + \Delta_{\text{mix}}(\phi \rightarrow f\bar{f}'), \quad (11)$$

$$\Delta_{\text{EW}}(\phi \rightarrow VV') = \frac{2\text{Re}[\Gamma_{\phi V V'}^{\text{1,tree}} \Gamma_{\phi V V'}^{\text{1,loop}*}]}{|\Gamma_{\phi V V'}^{\text{1,tree}}|^2} + \frac{\text{Re}[\Gamma_{\phi V V'}^{\text{1,tree}} \Gamma_{\phi V V'}^{\text{2,loop}*}]}{|\Gamma_{\phi V V'}^{\text{1,tree}}|^2} \frac{(1 - x_V - x_{V'})\lambda(x_V, x_{V'})}{\lambda(x_V, x_{V'}) + 12x_V x_{V'}} - \text{Re}\hat{\Pi}'_{VV}(m_V^2) - \text{Re}\hat{\Pi}'_{V'V'}(m_{V'}^2), \quad (12)$$

$$\Delta_{\text{EW}}(\phi \rightarrow V\phi') = \frac{2\text{Re}[\Gamma_{\phi V \phi'}^{\text{tree}} \Gamma_{\phi V \phi'}^{\text{loop}*}]}{|\Gamma_{\phi V \phi'}^{\text{tree}}|^2} - \text{Re}\hat{\Pi}'_{VV}(m_V^2) + \Delta_{\text{mix}}(\phi \rightarrow V\phi'), \quad (13)$$

$$\Delta_{\text{EW}}(\phi \rightarrow \phi'\phi'') = \frac{2\text{Re}[\Gamma_{\phi \phi' \phi''}^{\text{tree}} \Gamma_{\phi \phi' \phi''}^{\text{loop}*}]}{|\Gamma_{\phi \phi' \phi''}^{\text{tree}}|^2} + \Delta_{\text{mix}}(\phi \rightarrow \phi'\phi''), \quad (14)$$

where

$$\Gamma_{\phi f f'}^{\text{loop}} = \Gamma_{\phi f f'}^{\text{S,loop}} + m_{f'} \Gamma_{\phi f f'}^{\text{V}_1, \text{loop}} - m_f \Gamma_{\phi f f'}^{\text{V}_2, \text{loop}} + (m_\phi^2 + m_f m_{f'} - m_f^2 - m_{f'}^2) \Gamma_{\phi f f'}^{\text{T,loop}}, \quad (15)$$

$$\tilde{\Gamma}_{\phi f f'}^{\text{loop}} = \Gamma_{\phi f f'}^{\text{P,loop}} - m_{f'} \Gamma_{\phi f f'}^{\text{A}_1, \text{loop}} - m_f \Gamma_{\phi f f'}^{\text{A}_2, \text{loop}} + (m_\phi^2 - m_f m_{f'} - m_f^2 - m_{f'}^2) \Gamma_{\phi f f'}^{\text{PT,loop}}. \quad (16)$$

The external-leg corrections to the on-shell gauge boson $\text{Re}\hat{\Pi}'_{VV}(m_V^2)$ appear in $\Delta_{\text{EW}}(\phi \rightarrow V\phi')$ and $\Delta_{\text{EW}}(\phi \rightarrow VV')$, because the residue of the self-energy for the on-shell weak gauge boson is not set to unity in the applied renormalization scheme for electroweak parameters (see, e.g.,

³ For the CP-odd Higgs boson and the charged Higgs bosons, the decay $\phi \rightarrow VV'$ specified as $A \rightarrow ZZ/W^+W^-$ and $H^\pm \rightarrow W^\pm Z$, respectively. Since they are loop-induced processes, the analytical expressions of the decay rates are presented by Eq. (19).

Ref. [24]). The correction factor $\Delta_{\text{mix}}(\phi \rightarrow XY)$ corresponds to the non-vanishing contributions from mixing self-energies between two boson states. This type of contribution arises if external lines contain the charged Higgs boson in the THDM, where $\hat{\Pi}_{H+G^-}(m_{H^\pm}^2) = 0$ is not imposed as the renormalization condition in our renormalization scheme [56]. The analytical expressions are given in Ref. [23] for $\Delta_{\text{mix}}(\phi \rightarrow f\bar{f}')$ and $\Delta_{\text{mix}}(\phi \rightarrow V\phi')$, and Appendix B for $\Delta_{\text{mix}}(\phi \rightarrow \phi'\phi'')$.

In Table III, we summarize the references giving the analytical expressions for 1PI vertices, counterterms, and real photon emissions, which are needed to compute the two-body decay rates of all the additional Higgs bosons.

For decay processes induced at loop levels, their decay rates are given at LO as

$$\Gamma(\phi \rightarrow V\gamma)_{\text{LO}} = \frac{(1-x_V)^3}{32\pi m_\phi(1+\delta_{V\gamma})} (|\hat{\Gamma}_{\phi V\gamma}^{2,\text{loop}}|^2 + |\hat{\Gamma}_{\phi V\gamma}^{3,\text{loop}}|^2), \quad (V = \gamma, Z, W^\pm) \quad (17)$$

$$\Gamma(\phi \rightarrow gg)_{\text{LO}} = \frac{1}{8\pi m_\phi} (|\hat{\Gamma}_{\phi gg}^{2,\text{loop}}|^2 + |\hat{\Gamma}_{\phi gg}^{3,\text{loop}}|^2). \quad (18)$$

In the above expression, we applied the Ward identity by which the contribution from $\hat{\Gamma}_{\phi XY}^{1,\text{loop}}$ is rewritten by $\hat{\Gamma}_{\phi XY}^{2,\text{loop}}$. If $\phi \rightarrow VV'$ decays appear at the one-loop level, e.g., $H^\pm \rightarrow W^\pm Z$ in the THDMs, the decay rate is expressed at LO as ^{4 5}

$$\Gamma(\phi \rightarrow VV')_{\text{LO}} = \frac{\lambda^{3/2}(x_V, x_{V'})}{64\pi m_\phi x_V x_{V'}} \left\{ |\hat{\Gamma}_{\phi VV'}^{1,\text{loop}}|^2 \left[1 + \frac{12x_V x_{V'}}{\lambda(x_V, x_{V'})} \right] + \frac{|\hat{\Gamma}_{\phi VV'}^{2,\text{loop}}|^2}{4} \lambda(x_V, x_{V'}) \right. \\ \left. + 2x_V x_{V'} |\hat{\Gamma}_{\phi VV'}^{3,\text{loop}}|^2 + \text{Re}[\hat{\Gamma}_{\phi VV'}^{1,\text{loop}} \hat{\Gamma}_{\phi VV'}^{2,\text{loop}*}] (1 - x_V - x_{V'}) \right\}. \quad (19)$$

The QCD corrections are included in the following processes,

$$\phi \rightarrow q\bar{q}', \quad \phi \rightarrow t\bar{t}, \quad \phi \rightarrow t\bar{b}, \quad \phi \rightarrow \gamma\gamma, \quad \phi \rightarrow Z\gamma, \quad \phi \rightarrow gg. \quad (20)$$

The evaluation of QCD corrections for the processes of Eq. (20) is common for all the models. In the following paragraphs, we briefly describe how the QCD corrections are included for each decay mode in H-COUP_3.0. See Ref. [12] for detailed expressions for these QCD corrections.

For the decays into light quarks $\phi \rightarrow q\bar{q}'$, the corrections up to next-to-next-to leading order (NNLO) are computed in the $\overline{\text{MS}}$ scheme [90–94]. The NNLO corrections involve top-quark loop contributions evaluated in the heavy top-quark mass limit $m_\phi \ll m_t$. For the decays including the top-quark $\phi \rightarrow t\bar{t}$ and $\phi \rightarrow t\bar{b}$, the dominant QCD corrections would depend on the size of the mass of additional Higgs bosons m_ϕ . If these masses are taken to be around the threshold region (e.g.,

⁴ If one specifies $\phi \rightarrow VV'$ as $H \rightarrow ZZ/W^+W^-$ in the HSM or the THDM, these processes realize at the tree level.

The analytical expressions are given by Eq. (8).

⁵ We note that, for the charged Higgs decays $H^\pm \rightarrow W^\pm Z$ in the THDM, $H^\pm G^\mp$ and $H^\pm W^\mp$ mixing contributions exist. They are included in $\hat{\Gamma}_{\phi VV'}^{1,\text{loop}}$.

Modes	1PI vertex	Counterterm	Real emission	Models
$H \rightarrow f\bar{f}$	[56]	[21]	[21]	HSM
$H \rightarrow W^+W^-$	[56]	[21]	[22]	HSM
$H \rightarrow ZZ$	[56]	[21]	-	HSM
$H \rightarrow AZ$	[22]	[22]	-	IDM
$H \rightarrow W^\pm H^\mp$	[23]	[23]	[23]	HSM
$H \rightarrow hh$	[21]	[21]	-	HSM
$H \rightarrow AA$	App. B	App. B	-	IDM ($h \rightarrow AA$ (App. B))
$H \rightarrow H^+H^-$	App. B	App. B	App. C	IDM ($h \rightarrow H^+H^-$ (App. B))
$H \rightarrow \gamma\gamma/Z\gamma/gg$	[56]	-	-	HSM
$A \rightarrow f\bar{f}$	[22]	[22]	[22]	-
$A \rightarrow Zh$	[22]	[22]	-	-
$A \rightarrow ZH$	[22]	[22]	-	IDM
$A \rightarrow W^\pm H^\mp$	[23]	[22]	[22]	IDM
$A \rightarrow \gamma\gamma/Z\gamma/gg/WW/ZZ$	[22]	-	-	-
$H^\pm \rightarrow f\bar{f}'$	[23]	[23]	[23]	-
$H^\pm \rightarrow W^\pm h$	[23]	[23]	[23]	-
$H^\pm \rightarrow W^\pm H/W^\pm A$	[23]	[23]	[23]	IDM
$H^\pm \rightarrow W^\pm Z$	[23]	[23]	-	-
$H^\pm \rightarrow W^\pm \gamma$	[23]	-	-	-

TABLE III. References for the expressions of each contribution to the decay rate in the THDMs. In Ref. [56], the expression for the h vertices is presented, so that the corresponding expression for the H vertices is obtained by taking the appropriate replacement of the coupling for h with the corresponding one for H . The column “Models” shows the possible other models to give the corresponding decay mode, which are implemented in H-COUP_3.0, i.e., the IDM and the HSM.

$m_{H,A} \sim 2m_t$ and $m_{H^\pm} \sim m_t + m_b$) the corrections with top-quark mass are important, which is evaluated at NLO in the on-shell scheme [95–97]. Conversely, if these are far above the threshold region (e.g., $m_{H,A} \gg 2m_t$ and $m_{H^\pm} \gg m_t + m_b$), the logarithmic contributions $\log(m_\phi^2/m_t^2)$ become important. One can evaluate the corrections including such logarithmic contributions up

to NNLO in the $\overline{\text{MS}}$ scheme in the same way as $\phi \rightarrow q\bar{q}$. Since in the intermediate region of m_ϕ , both above contributions could have a large influence, we interpolate them according to Ref. [98].

We evaluate QCD corrections to $\phi \rightarrow \gamma\gamma$ [99–101] and $\phi \rightarrow Z\gamma$ [96] at NLO. While the analytical formulae of the former can be applied to any mass region of additional Higgs bosons, those in the heavy top-quark limit are applied to the latter. To moderate these corrections, we choose the renormalization scale $\mu = m_\phi/2$ only for $\phi \rightarrow \gamma\gamma$ and $\phi \rightarrow Z\gamma$ ($\mu = m_\phi$ is used for the other processes.). For $\phi \rightarrow gg$, the corrections are calculated up to NNLO. The NLO corrections are composed of the virtual gluon loop corrections and the real emissions $\phi \rightarrow ggg$ and $\phi \rightarrow gq\bar{q}$. Following Ref. [101], we implement these contributions evaluated in the heavy top-quark limit. We neglect the remaining contributions for the real emissions, which are generally smaller than the virtual corrections (see the detail in Ref. [100]). For the NNLO QCD corrections to $\phi \rightarrow gg$, we use the formula evaluated in the heavy top-quark limit [102, 103].

As described above, some of the QCD corrections are computed by taking the heavy top-quark limit. However, additional Higgs bosons can be heavier than the top-quark, so that the QCD corrections derived in the heavy top-quark limit might be unreliable in the case of $m_\phi \gtrsim m_t$. For instance, the top-quark loop contributions to $\phi \rightarrow q\bar{q}$ contain the logarithmic contributions $\log(m_\phi^2/m_t^2)$, which gives sizable contributions in the case of $m_\phi \gg m_t$. Hence, we only include the contributions given in the heavy top-quark limit, i.e., the top-loop contributions to $\phi \rightarrow q\bar{q}$, the real emission contributions at NLO to $\phi \rightarrow gg$ and the NNLO corrections to $\phi \rightarrow gg$ in the evaluation of the QCD corrections if an additional Higgs boson is lighter than the top-quark ($m_\phi < m_t$).

Apart from the QCD correction factor $\Delta_{\text{QCD}}(\phi \rightarrow XY)$, quark masses coming from the Yukawa couplings are replaced by the running quark masses in $\Gamma_{\text{LO}}(\phi \rightarrow XY)$ for all the processes in Eq. (20).

The decays into an off-shell gauge boson $\phi \rightarrow VV^* \rightarrow Vff$ and $\phi \rightarrow \phi'V^* \rightarrow \phi'ff$ can happen in the case of $m_\phi < 2m_V$ for the former and $m_\phi < m_{\phi'} + m_V$ for the latter. While they are evaluated at electroweak LO ⁶, we incorporate NLO QCD corrections to them [104] in H-COUP_3.0.

IV. PROGRAM DESCRIPTION

One can download H-COUP_3.0 and the previous versions from the following web page,

<http://www-het.phys.sci.osaka-u.ac.jp/~hcoup>.

⁶ For the off-shell decays of the 125 GeV Higgs boson h , $h \rightarrow VV^* \rightarrow Vff$, the NLO electroweak corrections are included.

In order to run the H-COUP program, a Fortran compiler (`gfortran` is recommended) and `LoopTools` [105] are required. The installation and running procedures are the same as H-COUP_2.0, and these are described in the previous manual [19], except for the procedure to specify the path of `LoopTools`. Open Makefile by an editor and replace `PATH_TO_libooptools_a` and `PATH_TO_looptools_h` appearing in the lines `LPATHa` and `LPATHh` with the correct paths to the `libooptools.a` and `looptools.h`, respectively. In the following, we briefly overview the structure of H-COUP_3.0 and explain the improvement from previous versions.

The H-COUP program is composed of three blocks; input, computation, and output blocks [18, 19]. In the input block, H-COUP_3.0 reads the input files in `$(HCOUP-3.0)/inputs`, where `$(HCOUP-3.0)` indicates a path of the HCOUP-3.0 directory. In H-COUP_3.0, the model and the order of calculations are specified in `in_main.txt`. This part is different from H-COUP_2.0, where one specifies them from the command line interface. The model IDs are defined as `HSM=1`, `THDM-I=2`, `THDM-II=3`, `THDM-X=4`, `THDM-Y=5`, and `IDM=6`. The order of electroweak corrections is specified by `LO=0` or `NLO=1`, while the order of QCD corrections are defined as `LO(quark mass:OS)=-1`, `LO(quark mass:MSbar)=0`, `NLO=1`, and `NLO=2`. The option, `LO(quark mass:OS)`, provides the LO results calculated with OS quark masses, while `LO(quark mass:MSbar)` performs LO calculation with $\overline{\text{MS}}$ quark masses. The detailed descriptions of the SM-like Higgs boson decays are given in Ref. [106]. For those of the heavy Higgs boson decays, see Refs. [21–23]. The example of the `in_main.txt` is shown in List. 1.

The model-independent parameters are read from the input files, `in_sm.txt` and `momentum.txt`. The SM parameters listed in Table IV are specified in `in_sm.txt`. The squared momenta of the renormalized form factors of the SM-like Higgs bosons are read from `momentum.txt`. The detailed descriptions of these parameters can be found in Refs. [18, 19]. If one changes the inputs in `in_sm.txt`, execute

\$ make clean

before numerical evaluations.

The model-dependent parameters in the HSM, THDM, and IDM are specified in `in_hsm.txt`, `in_thdm.txt`, and `in_idm.txt`, respectively. The input parameters and their default values are summarized in Tables V, VI, and VII. The cutoff scale Λ is used for the theoretical constraints, such as triviality and vacuum stability bounds. In addition, we have newly introduced the renormalization scale μ_r , which is used to fix the $\overline{\text{MS}}$ renormalized quantities. In the HSM and THDM, we have the `SCHEME` option, which specifies the renormalization scheme of the tadpole and dimensionful parameters, which was discussed in Sec. III. The example of the `in_hsm.txt` is shown

Parameter	Definition in H-COUP	Description	Default value
α_{em}	<code>alpha_em</code>	Fine structure constant	137.035999084^{-1}
m_Z	<code>mz</code>	Z mass	91.1876 GeV
G_F	<code>G_F</code>	Fermi constant	1.1663788×10^{-5} GeV $^{-2}$
$\Delta\alpha_{\text{em}}$	<code>del_alpha</code>	Shift of α_{em}	0.06627
$\alpha_s(m_Z)$	<code>alpha_s</code>	Strong coupling	0.1179
m_h	<code>mh</code>	Higgs boson mass	125.25 GeV
m_t	<code>mt</code>	On-shell t mass	172.5 GeV
m_b	<code>mb</code>	On-shell b mass	4.78 GeV
m_c	<code>mc</code>	On-shell c mass	1.67 GeV
$\overline{m}_b(m_b)$	<code>mb_ms</code>	$\overline{\text{MS}}$ b mass	4.18 GeV
$\overline{m}_c(m_c)$	<code>mc_ms</code>	$\overline{\text{MS}}$ c mass	1.27 GeV
m_τ	<code>mtau</code>	τ mass	1.77686 GeV
m_μ	<code>mmu</code>	μ mass	0.1056583755 GeV

TABLE IV. Input global SM parameters. All these parameters are defined by double precision. All input values are taken from particle data group [107].

in List. 2.

In the computation block, H-COUP_3.0 calculates the decay rates of any Higgs bosons in the specified model at a given order of calculations, where the evaluation of the loop functions are performed with `LoopTools` [105]. The possible decay modes of the additional Higgs bosons are listed in Table III⁷.

In the output block, H-COUP_3.0 creates output files in `$HCOUP-3.0/outputs`. In addition to the `out_sm.txt`, `outGamma_sm.txt` and `outBR_sm.txt`, one has the output files for specifying models, e.g., `out_hsm.txt`, `outGamma_hsm.txt` and `outBR_hsm.txt` for the HSM. In the following, we represent them as `out_xx.txt`, `outGamma_xx.txt`, and `outBR_xx.txt` for simplicity. In `out_xx.txt`, the values of the renormalized form factors are listed. The predictions for the partial decay rates of Higgs bosons and their total widths are given in `outGamma_xx.txt` with the values of the input parameters. Similarly, the predictions for the decay branching ratios are given in `outBR_xx.txt`. One can check whether a given parameter set is allowed or excluded under the constraints, such as perturbative unitarity, vacuum stability, triviality, true vacuum conditions, and/or electroweak precision tests. The examples of `outGamma_hsm.txt` and `outBR_hsm.txt` are shown in Lists. 3 and

⁷ In several modes such as $H \rightarrow hh$ in the THDM, partial decay widths would take negative values depending on the input parameters due to the truncation of two-loop effects (see Refs. [21–23]). In the current version, we simply output negative values showing a warning message in a command line interface.

	HSM							
Parameters	m_H	α	μ_S	λ_S	$\lambda_{\Phi S}$	Λ	μ_R	Scheme
H-COUP def.	mbh	alpha	mu_s	lam_s	lam_phis	cutoff	mu_r	SCHEME
Default value	500 GeV	0.1	0	0.1	0	3 TeV	500 GeV	0

TABLE V. Input parameters in the HSM. All parameters are defined by double precision.

	THDM									
Parameters	m_{H^\pm}	m_A	m_H	M^2	$s_{\beta-\alpha}$	$\text{Sign}(c_{\beta-\alpha})$	$\tan\beta$	Λ	μ_R	Scheme
H-COUP def.	mch	ma	mbh	bmsq	sin_ba	sign	tanb	cutoff	mu_r	SCHEME
Default value	500 GeV	500 GeV	500 GeV	(450 GeV) ²	1	1	1.5	3 TeV	500 GeV	0

TABLE VI. Input parameters in the THDMs. All parameters are defined by double precision except for sign which is defined by an integer and can be either 1 or -1 .

	IDM							
Parameters	m_{H^\pm}	m_A	m_H	μ_2^2	λ_2	Λ	μ_R	
H-COUP def.	mch	ma	mbh	mu2sq	lam2	cutoff	mu_r	
Default value	500 GeV	500 GeV	500 GeV	(500 GeV) ²	0.1	3 TeV	500 GeV	

TABLE VII. Input parameters in the IDM. All parameters are defined by double precision.

4, which are calculated by using the inputs given in Lists. 1 and 2.

Listing 1. Example of the input file (in_main.txt)

```

1 !=====!
2 !
3 ! Input parameters for main      !
4 !
5 !=====!
6
7 1      ! Model ID: 1 = HSM, 2 = THDM-I, 3 = THDM-II, 4 = THDM-X, 5 = THDM-Y, 6 =
      IDM
8 1      ! Order of EW: 0 = LO, 1 = NLO
9 2      ! Order of QCD: -1 = LO(quark mass:OS), 0 = LO(quark mass:MSbar), 1 = NLO,
      2 = NNLO

```

Listing 2. Example of the input file (in_hsm.txt)

```

1 !=====!
2 !
3 ! Input parameters for the HSM    !
4 !
5 !=====!
6
7 500.d0      ! m_H in GeV
8 0.1d0       ! alpha
9 0.d0        ! lambda_{phi S}
10 0.1d0      ! lambda_S
11 0.d0       ! mu_S in GeV
12 3.d3       ! cutoff in GeV

```

```

13 400.d0          ! MSbar renormalization scale in GeV
14 0              ! 0: Pinched tadpole, 1: KOSY with PT

```

Listing 3. Example of the output file (outGamma_hsm.txt)

```

=====
1 #=====
2 #
3 #           H-COUP [Version 3.0 (November 28, 2023)]
4 #           Program for full-NLO predictions of any Higgs-boson decays
5 #           in non-minimal Higgs models
6 #
7 #           \protect\vrule width0pt\protect\href{http://www-het.phys.sci.osaka-u
           .ac.jp/\string~hcoup}{http://www-het.phys.sci.osaka-u.ac.jp/\$sim$hcoup}
8 #
9 #=====
10 BLOCK MODEL #
11 1 1 # HSM
12 2 0 # MSbar renormalization scheme
13 BLOCK BSMINPUTS #
14 1 1.00000000E-01 # alpha
15 2 0.00000000E+00 # lambda_{phi S}
16 3 1.00000000E-01 # lambda_S
17 4 0.00000000E+00 # mu_S (GeV)
18 5 5.00000000E+02 # mu_r (GeV)
19 BLOCK SMINPUTS #
20 1 7.29735257E-03 # alpha_em
21 2 1.16637880E-05 # Fermi constant
22 3 1.17900000E-01 # alpha_s
23 4 1.27000000E+00 # mc(mc) MSbar
24 5 4.18000000E+00 # mb(mb) MSbar
25 6 1.67000000E+00 # mc On-shell
26 7 4.78000000E+00 # mb On-shell
27 BLOCK MASS #
28 4 6.79114206E-01 # mc(mh) MSbar
29 5 2.85835750E+00 # mb(mh) MSbar
30 6 1.72500000E+02 # mt
31 13 1.05658375E-01 # mmu
32 15 1.77686000E+00 # mtau
33 23 9.11876000E+01 # mz
34 24 8.09388642E+01 # mw (calculated,tree)
35 24 8.04085771E+01 # mw (calculated,1-loop)
36 25 1.25250000E+02 # mh
37 35 5.00000000E+02 # mH
38 BLOCK CONSTRAINTS #
39 0 3.00000000E+03 # The cutoff scale (GeV)
40 1 0 # Vacuum stability at tree level [0=OK, 1=No]
41 2 0 # Tree-level unitarity [0=OK, 1=No]
42 3 0 # S and T parameters [0=OK, 1=No]
43 4 0 # True vacuum [0=OK, 1=No]
44 5 0 # Vacuum stability (RGE improved with the cutoff scale) [0=OK, 1=
           No]
45 6 0 # Triviality (with the cutoff scale) [0=OK, 1=No]
46 #
47 # Partial decay widths of the SM-like Higgs boson by H-COUP #
48 #           PDG           Width
49 DECAY      25           0.40743346E-02 # EW:NLO QCD:NNLO
50 #           Gamma      NDA      ID1      ID2
51 1.42029147E-04 2 4 -4 # Gamma(h -> c c~)
52 2.45364374E-03 2 5 -5 # Gamma(h -> b b~)
53 8.82215414E-07 2 13 -13 # Gamma(h -> mu- mu+)
54 2.54256192E-04 2 15 -15 # Gamma(h -> tau- tau+)
55 3.32918565E-04 2 21 21 # Gamma(h -> g g)
56 9.25841223E-06 2 22 22 # Gamma(h -> gam gam)
57 6.47474306E-06 2 22 23 # Gamma(h -> gam Z)
58 9.00793124E-05 2 23 23 # Gamma(h -> Z Z*)
59 7.84792254E-04 2 24 -24 # Gamma(h -> W+ W-*)
60 #
61 # Partial decay widths of the additional CP-even Higgs boson bH by H-COUP #

```

62 #	PDG	Width			
63	DECAY 35	0.87367479E+00	# EW:NLO	QCD:NNLO	
64 #	Gamma	NDA	ID1	ID2	
65	1.11119396E-01	2	6	-6	# Gamma(bH -> t t~)
66	7.77390858E-05	2	5	-5	# Gamma(bH -> b b~)
67	4.42785519E-06	2	4	-4	# Gamma(bH -> c c~)
68	3.52102715E-08	2	13	-13	# Gamma(bH -> mu- mu+)
69	1.01600689E-05	2	15	-15	# Gamma(bH -> tau- tau+)
70	1.72174523E-01	2	23	23	# Gamma(bH -> Z Z)
71	3.62420028E-01	2	24	-24	# Gamma(bH -> W+ W-)
72	2.27571695E-01	2	25	25	# Gamma(bH -> h h)
73	2.91017661E-04	2	21	21	# Gamma(bH -> g g)
74	2.62532767E-07	2	22	22	# Gamma(bH -> gam gam)
75	5.50566818E-06	2	22	23	# Gamma(bH -> gam Z)

Listing 4. Example of the output file (outBR_hsm.txt)

```

1 #=====
2 #
3 #           H-COUP [Version 3.0 (November 28, 2023)]
4 #           Program for full-NLO predictions of any Higgs-boson decays
5 #           in non-minimal Higgs models
6 #
7 #           \protect\vrule widthOpt\protect\href{http://www-het.phys.sci.osaka-u
      .ac.jp/\string~hcoup}{http://www-het.phys.sci.osaka-u.ac.jp/\sim$hcoup}
8 #
9 #=====
10 BLOCK MODEL #
11     1     1     # HSM
12     2     0     # MSbar renormalization scheme
13 BLOCK BSMINPUTS #
14     1     1.00000000E-01 # alpha
15     2     0.00000000E+00 # lambda_{phi S}
16     3     1.00000000E-01 # lambda_S
17     4     0.00000000E+00 # mu_S (GeV)
18     5     5.00000000E+02 # mu_r (GeV)
19 BLOCK SMINPUTS #
20     1     7.29735257E-03 # alpha_em
21     2     1.16637880E-05 # Fermi constant
22     3     1.17900000E-01 # alpha_s
23     4     1.27000000E+00 # mc(mc) MSbar
24     5     4.18000000E+00 # mb(mb) MSbar
25     6     1.67000000E+00 # mc On-shell
26     7     4.78000000E+00 # mb On-shell
27 BLOCK MASS #
28     4     6.79114206E-01 # mc(mh) MSbar
29     5     2.85835750E+00 # mb(mh) MSbar
30     6     1.72500000E+02 # mt
31     13    1.05658375E-01 # mmu
32     15    1.77686000E+00 # mtau
33     23    9.11876000E+01 # mz
34     24    8.09388642E+01 # mw (calculated,tree)
35     24    8.04085771E+01 # mw (calculated,1-loop)
36     25    1.25250000E+02 # mh
37     35    5.00000000E+02 # mH
38 BLOCK CONSTRAINTS #
39     0     3.00000000E+03 # The cutoff scale (GeV)
40     1     0     # Vacuum stability at tree level [0=OK, 1=No]
41     2     0     # Tree-level unitarity [0=OK, 1=No]
42     3     0     # S and T parameters [0=OK, 1=No]
43     4     0     # True vacuum [0=OK, 1=No]
44     5     0     # Vacuum stability (RGE improved with the cutoff scale) [0=OK, 1=
45           No]
46     6     0     # Triviality (with the cutoff scale) [0=OK, 1=No]
47 # Decay branching ratios of the SM-like Higgs boson by H-COUP #
48 #           PDG           Width
49 DECAY 25     0.40743346E-02 # EW:NLO QCD:NNLO

```

50 #	BR	NDA	ID1	ID2	
51	3.48594707E-02	2	4	-4	# BR(h -> c c~)
52	6.02219501E-01	2	5	-5	# BR(h -> b b~)
53	2.16529938E-04	2	13	-13	# BR(h -> mu- mu+)
54	6.24043478E-02	2	15	-15	# BR(h -> tau- tau+)
55	8.17111502E-02	2	21	21	# BR(h -> g g)
56	2.27237407E-03	2	22	22	# BR(h -> gam gam)
57	1.58915350E-03	2	22	23	# BR(h -> gam Z)
58	2.21089630E-02	2	23	23	# BR(h -> Z Z*)
59	1.92618509E-01	2	24	-24	# BR(h -> W+ W-*)
60 #					
61 #	Decay branching ratios of the additional CP-even Higgs boson bH by H-COUP #				
62 #	PDG	Width			
63 DECA	35	0.87367479E+00	#	EW:NLO	QCD:NNLO
64 #	BR	NDA	ID1	ID2	
65	1.27186222E-01	2	6	-6	# BR(bH -> t t~)
66	8.89794312E-05	2	5	-5	# BR(bH -> b b~)
67	5.06808167E-06	2	4	-4	# BR(bH -> c c~)
68	4.03013477E-08	2	13	-13	# BR(bH -> mu- mu+)
69	1.16291199E-05	2	15	-15	# BR(bH -> tau- tau+)
70	1.97069350E-01	2	23	23	# BR(bH -> Z Z)
71	4.14822577E-01	2	24	-24	# BR(bH -> W+ W-)
72	2.60476436E-01	2	25	25	# BR(bH -> h h)
73	3.33096095E-04	2	21	21	# BR(bH -> g g)
74	3.00492552E-07	2	22	22	# BR(bH -> gam gam)
75	6.30173635E-06	2	22	23	# BR(bH -> gam Z)

V. EXAMPLES OF NUMERICAL EVALUATIONS

As mentioned in Introduction, it is quite important to include radiative corrections to the analyses for the synergy between the precise measurements of h and the direct searches for additional Higgs bosons in order to test and discriminate the extended Higgs models. We here show an example of such analyses by using H-COUP_3.0.

In Fig. 2, we show the correlation between the decay branching ratio of the $A \rightarrow Zh$ process and the deviation of the decay rate of $h \rightarrow ZZ^*$ from the SM prediction in the Type-I THDM. We define $\Delta R(h \rightarrow ZZ^*) \equiv \Gamma[h \rightarrow ZZ^*]/\Gamma_{\text{SM}}[h \rightarrow ZZ^*]$ to parameterize the deviation [22]. We take $m_A = m_H = 300$ GeV and $\tan\beta = 2$, while the values of $\sin(\beta - \alpha)$ and M^2 are scanned under the constraints of the perturbative unitarity, the vacuum stability and the electroweak S and T parameters. We also take into account the constraints from flavor measurements, direct search results of additional Higgs bosons and Higgs coupling measurements. The left panel and the right panel show results with $\cos(\beta - \alpha) < 0$ and $\cos(\beta - \alpha) > 0$, respectively. Black curves represent tree-level predictions, while the color dots show the results including radiative corrections with different colors denoting those given by different values of M^2 . It is clearly seen that the radiative corrections significantly change the correlation predicted at LO. In particular, the case with smaller values of M^2 show the larger difference between the results at LO and NLO, because of the larger non-decoupling loop effects of the additional Higgs bosons.

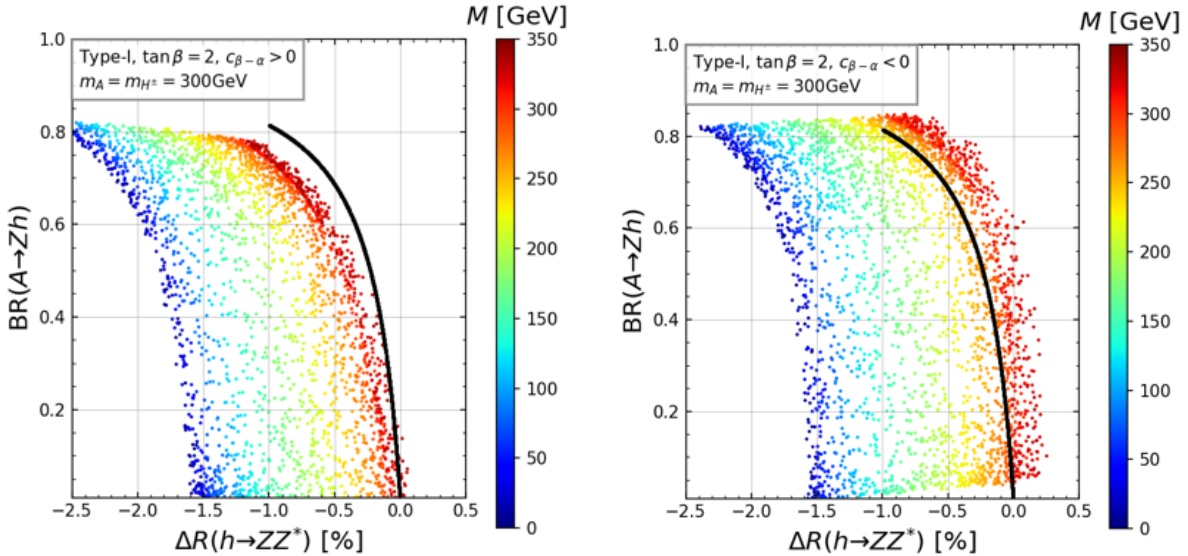


FIG. 2. The correlation between decay branching ratios of the $A \rightarrow Zh$ process in the Type-I THDM and the deviation of the decay rate of $h \rightarrow ZZ$ in the Type-I THDM from that in the SM [22].

In addition to this particular example, it has been known that radiative corrections can significantly change the other correlations, e.g., the $H \rightarrow hh$ decay rate and the triple Higgs boson coupling hhh [21], which can also be evaluated by using H-COUP_3.0. Therefore, H-COUP_3.0 can realize the synergy analysis discussed above in a more robust way, by which we can reconstruct the structure of the Higgs sector.

VI. SUMMARY

We have provided the manual for the H-COUP_3.0 program which is a set of Fortran codes for numerical calculations of decay rates of all the Higgs bosons at NLO in electroweak interactions with QCD corrections in the HSM, four types of THDMs and the IDM. The electroweak corrections are evaluated based on the gauge independent on-shell renormalization scheme. We have described the renormalization schemes, the renormalized vertex functions and the radiatively corrected decay rates for the processes $\phi \rightarrow \phi'\phi''$, $\phi \rightarrow V\phi'$, $\phi \rightarrow VV'$ and $\phi \rightarrow f\bar{f}'$, which are implemented in H-COUP_3.0. We also have discussed the loop induced decays; i.e. $\phi \rightarrow V\gamma$, $\phi \rightarrow gg$ and $\phi \rightarrow W^\pm Z$, which can be evaluated at LO in electroweak interactions in H-COUP_3.0. We have designed the program in a way that the user can choose the different two (four) renormalization schemes for the tadpole in the HSM (THDMs), among which the decay rate of $\phi \rightarrow \phi'\phi''$ can be different. We then

have explained the structure of the program, and have shown the examples of the input and output files. Finally, we have demonstrated the analysis by using H-COUP_3.0. As an example, we have shown the loop-corrected correlation between the branching ratio of $A \rightarrow Zh$ and the deviation in the $h \rightarrow ZZ^*$ decay in the Type-I THDM.

ACKNOWLEDGMENTS

This work is supported in part by the Grant-in-Aid on Innovative Areas, the Ministry of Education, Culture, Sports, Science and Technology, No. 20H00160 and No. 23K17691 [S.K.], JSPS KAKENHI Grant No. 23KJ0086 and the National Science Centre, Poland, under research Grant No. 2020/38/E/ST2/00243 [K.S.], Early-Career Scientists, No. 20K14474 [M.K.] and JSPS KAKENHI Grant No. 22KJ3126 [M.A.].

Appendix A: Scheme difference for $\overline{\text{MS}}$ parameters in THDMs

We calculate the scheme difference for hhh , Hhh , HAA , and HH^+H^- vertices in THDMs. We focus on the four schemes presented in Sec. III. The difference between two schemes is defined by

$$\Delta\Gamma(\text{ABC} - \text{A'B'C'}) \equiv \Gamma(\text{ABC}) - \Gamma(\text{A'B'C'}). \quad (\text{A1})$$

In Appendix, the trigonometric functions $\sin\theta$ and $\cos\theta$ are represented using the shorthand notation as s_θ and c_θ .

As discussed in the main text, the counterterms δM^2 and δm_{12}^2 are defined in the $\overline{\text{MS}}$ scheme. Analytical expressions for these counterterms are derived in the following way. The counterterms δM^2 or δm_{12}^2 absorb the remnant of the UV divergence of the renormalized hhh vertex without these counterterms. In the KOSY1 scheme, this condition yields [56]

$$\begin{aligned} \frac{\delta M^2}{M^2} \Big|_{\text{KOSY1}} &= \frac{1}{16\pi^2 v^2} \left[2 \sum_f N_c^f m_f^2 \zeta_f^2 + 4M^2 - 2m_{H^\pm}^2 - m_A^2 \right. \\ &\quad \left. + \frac{s_{2\alpha}}{s_{2\beta}} (m_H^2 - m_h^2) - 3(2m_W^2 + m_Z^2) \right] \Delta_{\text{div}}, \end{aligned} \quad (\text{A2})$$

where Δ_{div} represents the divergent part given by $\Delta_{\text{div}} = 1/\epsilon - \gamma_E + \log 4\pi$. Definitions and the explicit expression of coupling factor ζ_f are given in Ref. [21].

In the PT1 scheme, additional UV divergent contributions in the scheme difference between KOSY1 and PT1 are absorbed by δM^2 [20],

$$\frac{\delta M^2}{M^2} \Big|_{\text{PT1}} = \frac{\delta M^2}{M^2} \Big|_{\text{KOSY1}} + \frac{2 c_{2\beta}}{v s_{2\beta}} \left(\frac{\Gamma_h^{1\text{PI}}}{m_h^2} c_{\beta-\alpha} - \frac{\Gamma_H^{1\text{PI}}}{m_H^2} s_{\beta-\alpha} \right)_{\text{div}}, \quad (\text{A3})$$

where “div.” denotes the UV divergent part. As shown in Ref. [20], the last term corresponds to the scheme difference between the KOSY scheme and the PT scheme in $\delta\beta$,

$$\Delta\delta\beta(\text{PT} - \text{KOSY}) = -\frac{1}{v} \left(\frac{\Gamma_h^{1\text{PI}}}{m_h^2} c_{\beta-\alpha} - \frac{\Gamma_H^{1\text{PI}}}{m_H^2} s_{\beta-\alpha} \right). \quad (\text{A4})$$

Thus, Eq. (A3) can be rewritten by

$$\frac{\delta M^2}{M^2} \Big|_{\text{PT1}} = \frac{\delta M^2}{M^2} \Big|_{\text{KOSY1}} - 2 \frac{c_{2\beta}}{s_{2\beta}} \Delta\delta\beta(\text{PT} - \text{KOSY})_{\text{div.}}. \quad (\text{A5})$$

From the definition of M^2 , i.e., $M^2 = m_{12}^2/(c_\beta s_\beta)$, the counterterm δm_{12}^2 in the KOSY2 scheme and the PT2 scheme are obtained from the KOSY1 scheme and the PT1 scheme by the replacement,

$$\delta M^2 \rightarrow M^2 \frac{\delta m_{12}^2}{m_{12}^2} - 2M^2 \frac{c_{2\beta}}{s_{2\beta}} \overline{\delta\beta}, \quad (\text{A6})$$

with $\overline{\delta\beta} = \delta\beta + \delta\beta^{\text{PT}}$ where $\delta\beta^{\text{PT}}$ is the pinch term contribution for $\delta\beta$. Requiring cancellation of the UV divergence in the hhh vertex, in the KOSY2 and PT2 schemes, one obtains

$$\frac{\delta m_{12}^2}{m_{12}^2} \Big|_{\text{KOSY2,PT2}} = \frac{\delta M^2}{M^2} \Big|_{\text{KOSY1}} + 2 \frac{c_{2\beta}}{s_{2\beta}} \delta\beta|_{\text{div.}}. \quad (\text{A7})$$

We note that δm_{12}^2 is common between KOSY2 and PT2 since there is no scheme difference (see e.g., Eq. (A9)). Also, note that there is no UV divergence in $\delta\beta^{\text{PT}}$. The differences among these schemes are evaluated as

$$\Delta\hat{\Gamma}_{hhh}(\text{PT1} - \text{KOSY1}) = -\frac{12M^2}{v^2} \frac{c_{2\beta} c_{\alpha+\beta} c_\beta^2}{s_{2\beta}^2} \left(\frac{\Gamma_h^{1\text{PI}}}{m_h^2} c_{\beta-\alpha} - \frac{\Gamma_H^{1\text{PI}}}{m_H^2} s_{\beta-\alpha} \right)_{\text{fin.}}, \quad (\text{A8})$$

$$\Delta\hat{\Gamma}_{hhh}(\text{PT2} - \text{KOSY2}) = 0, \quad (\text{A9})$$

$$\begin{aligned} \Delta\hat{\Gamma}_{Hhh}(\text{PT1} - \text{KOSY1}) &= -\frac{4M^2}{v^2} \frac{c_{2\beta} c_{\beta-\alpha}}{s_{2\beta}^2} (3s_\alpha c_\alpha - s_\beta c_\beta) \\ &\quad \times \left(\frac{\Gamma_h^{1\text{PI}}}{m_h^2} c_{\beta-\alpha} - \frac{\Gamma_H^{1\text{PI}}}{m_H^2} s_{\beta-\alpha} \right)_{\text{fin.}}, \end{aligned} \quad (\text{A10})$$

$$\Delta\hat{\Gamma}_{Hhh}(\text{PT2} - \text{KOSY2}) = 0, \quad (\text{A11})$$

$$\Delta\hat{\Gamma}_{HAA}(\text{PT1} - \text{KOSY1}) = -\frac{M^2}{v^2} \frac{c_{2\beta}}{s_\beta^2} \frac{s_{\alpha+\beta}}{c_\beta^2} \left(\frac{\Gamma_h^{1\text{PI}}}{m_h^2} c_{\beta-\alpha} - \frac{\Gamma_H^{1\text{PI}}}{m_H^2} s_{\beta-\alpha} \right)_{\text{fin.}}, \quad (\text{A12})$$

$$\Delta\hat{\Gamma}_{HAA}(\text{PT2} - \text{KOSY2}) = 0, \quad (\text{A13})$$

$$\Delta\hat{\Gamma}_{HH+H-}(\text{PT1} - \text{KOSY1}) = \Delta\hat{\Gamma}_{HAA}(\text{PT1} - \text{KOSY1}), \quad (\text{A14})$$

$$\Delta\hat{\Gamma}_{HH+H-}(\text{PT2} - \text{KOSY2}) = 0, \quad (\text{A15})$$

where “fin.” denotes the finite part. We note that Eq. (A14) is obtained from the fact that one holds $\Delta\delta C_{H^\pm}(\text{PT1} - \text{KOSY1}) = 0$.

Appendix B: Renormalized $\phi\phi'\phi''$ vertex

In this section, we give formulae of $\Gamma_{\phi\phi'\phi''}^{\text{loop}}$, of several scalar three-point vertices in the THDM and the IDM, which is defined in Eq. (5) in Sec. III.

1. HAA and HH^+H^- vertices in the THDM

First, we show formulae for the HAA and HH^+H^- vertices in the THDM. We here give the formulas for the KOSY1 scheme defined in Sec. III. Conversions to other schemes are explained in the previous section.

Counterterms for the HAA and the HH^+H^- vertices in the THDM are expressed as

$$\delta\Gamma_{HAA} = 2\delta\lambda_{HAA} + 2\lambda_{HAA}(\delta Z_A + \frac{1}{2}\delta Z_H) + 2\lambda_{hAA}(\delta C_h - \delta\alpha) + 2\lambda_{HAG}(\delta C_A + \delta\beta), \quad (\text{B1})$$

$$\begin{aligned} \delta\Gamma_{HH^+H^-} &= \delta\lambda_{HH^+H^-} + \lambda_{HH^+H^-}(\delta Z_{H^+} + \frac{1}{2}\delta Z_H) + \lambda_{hH^+H^-}(\delta C_h - \delta\alpha) \\ &\quad + 2\lambda_{HH^+G^-}(\delta C_{H^\pm} + \delta\beta), \end{aligned} \quad (\text{B2})$$

with

$$\delta\lambda_{HAA} = -\frac{\lambda_{HAA}}{v}\delta v - \frac{c_{\beta-\alpha}}{v}\delta m_A^2 - \frac{s_{\alpha-3\beta} + 3s_{\alpha+\beta}}{8vs_\beta c_\beta}\delta m_H^2 + \frac{s_{\alpha+\beta}}{2vs_\beta c_\beta}\delta M^2 + G_\alpha^A \overline{\delta\alpha} + G_\beta^A \overline{\delta\beta}, \quad (\text{B3})$$

$$\delta\lambda_{HH^+H^-} = 2\delta\lambda_{HAA} \quad (A \rightarrow H^\pm). \quad (\text{B4})$$

In Eq. (B3), the factors G_α^ϕ and G_β^ϕ are expressed as

$$G_\alpha^\phi = -\frac{1}{8vs_\beta c_\beta} [c_{\alpha-3\beta}m_H^2 + c_{\alpha+\beta}(3m_H^2 - 4M^2) + 8s_{\beta-\alpha}s_\beta c_\beta m_\phi^2], \quad (\text{B5})$$

$$G_\beta^\phi = \frac{1}{8vs_\beta^2} [(2m_\phi^2 - m_H^2)s_{\alpha-5\beta} + 2(2m_\phi^2 - 7m_H^2 + 6M^2)s_{\beta-\alpha} + (2m_\phi^2 + 3m_H^2 - 4M^2)s_{\alpha+3\beta}]. \quad (\text{B6})$$

The analytic expressions for 1PI diagram contributions to the HAA and HH^+H^- vertices are given by

$$(16\pi^2) \Gamma_{HAA,F}^{\text{1PI}}[p_1^2, p_2^2, q^2] = -8\kappa_f^H \zeta_f^2 N_c^f \frac{m_f^4}{v^3} (B_0[q^2; m_f, m_f] + p_1 \cdot p_2 C_0[m_f, m_f, m_f]), \quad (\text{B7})$$

$$\begin{aligned} (16\pi^2) \Gamma_{HH^+H^-,F}^{\text{1PI}}[p_1^2, p_2^2, q^2] &= \\ & -\frac{4m_f^2}{v^3} N_c^f \kappa_f^H \left\{ 2(m_f^2 \zeta_f^2 + m_{f'}^2 \zeta_{f'}^2 - m_{f'}^2 \zeta_f \zeta_{f'}) \left(p_1^2 C_{21} + p_2^2 C_{22} + 2p_1 \cdot p_2 C_{23} + 4C_{24} - \frac{1}{2} \right) \right. \end{aligned}$$

$$\begin{aligned}
& + (m_f^2 \zeta_f^2 + m_{f'}^2 \zeta_{f'}^2) [(2p_1^2 + p_1 \cdot q)C_{11} + (2p_1 \cdot p_2 + p_2 \cdot q)C_{12} + p_1 \cdot qC_0] \\
& - 2m_{f'}^2 \zeta_f \zeta_{f'} (p_1 \cdot qC_{11} + p_2 \cdot qC_{12} + m_f^2 C_0) \Big\} [f, f', f], \tag{B8}
\end{aligned}$$

$$\begin{aligned}
& (16\pi^2) \Gamma_{HAA,B}^{\text{PI}} [p_1^2, p_2^2, q^2] = \\
& \frac{g^4}{4} v c_{\beta-\alpha} (4B_0[q^2; W, W] - 2) + \frac{g_Z^4}{8} v c_{\beta-\alpha} (4B_0[q^2; Z, Z] - 2) \\
& - \frac{g^4}{4} v c_{\beta-\alpha} C_{VSV}^{\phi\phi\phi} [W, H^\pm, W] - \frac{g_Z^4}{8} v c_{\beta-\alpha}^3 C_{VSV}^{\phi\phi\phi} [Z, h, Z] - \frac{g_Z^4}{8} v s_{\beta-\alpha}^2 c_{\beta-\alpha} C_{VSV}^{\phi\phi\phi} [Z, H, Z] \\
& - \frac{g^2}{2} c_{\beta-\alpha} \frac{m_A^2 - m_{H^\pm}^2}{v} C_{VSS}^{\phi\phi\phi} [W, H^\pm, G^\pm] + \frac{g^2}{2} \lambda_{HH+H-} C_{SVS}^{\phi\phi\phi} [H^\pm, W, H^\pm] \\
& - \frac{g^2}{2} c_{\beta-\alpha} \frac{m_A^2 - m_{H^\pm}^2}{v} C_{SSV}^{\phi\phi\phi} [G^\pm, H^\pm, W] - \frac{g_Z^2}{4} c_{\beta-\alpha}^2 \lambda_{hAG} C_{VSS}^{\phi\phi\phi} [Z, h, G] \\
& + \frac{g_Z^2}{4} s_{\beta-\alpha} c_{\beta-\alpha} \lambda_{HAG} C_{VSS}^{\phi\phi\phi} [Z, H, G] + \frac{g_Z^2}{2} s_{\beta-\alpha} c_{\beta-\alpha} \lambda_{hAA} C_{VSS}^{\phi\phi\phi} [Z, h, A] - \frac{g_Z^2}{2} s_{\beta-\alpha}^2 \lambda_{HAA} C_{VSS}^{\phi\phi\phi} [Z, H, A] \\
& + \frac{g_Z^2}{2} c_{\beta-\alpha}^2 \lambda_{Hhh} C_{SVS}^{\phi\phi\phi} [h, Z, h] - \frac{g_Z^2}{2} s_{\beta-\alpha} c_{\beta-\alpha} \lambda_{HHh} \{C_{SVS}^{\phi\phi\phi} [h, Z, H] + C_{SVS}^{\phi\phi\phi} [H, Z, h]\} \\
& + \frac{3g_Z^2}{2} s_{\beta-\alpha}^2 \lambda_{HHH} C_{SVS}^{\phi\phi\phi} [H, Z, H] - \frac{g_Z^2}{4} c_{\beta-\alpha}^2 \lambda_{hAG} C_{SSV}^{\phi\phi\phi} [G, h, Z] + \frac{g_Z^2}{4} s_{\beta-\alpha} c_{\beta-\alpha} \lambda_{HAG} C_{SSV}^{\phi\phi\phi} [G, H, Z] \\
& + \frac{g_Z^2}{2} s_{\beta-\alpha} c_{\beta-\alpha} \lambda_{hAA} C_{SSV}^{\phi\phi\phi} [A, h, Z] - \frac{g_Z^2}{2} s_{\beta-\alpha}^2 \lambda_{HAA} C_{SSV}^{\phi\phi\phi} [A, H, Z] \\
& + 2\lambda_{HH+H-} \lambda_{AAH+H-} B_0[q^2; H^\pm, H^\pm] + 4\lambda_{HH\pm G^\mp} \lambda_{AAH^\mp G^\pm} B_0[q^2; H^\pm, G^\pm] \\
& + 2\lambda_{AH^\pm G^\mp} \lambda_{AHH^\mp G^\pm} B_0[p_2^2; H^\pm, G^\pm] + 2\lambda_{AH^\pm G^\mp} \lambda_{AHH^\mp G^\pm} B_0[p_1^2; H^\pm, G^\pm] \\
& + 2\lambda_{HG^\pm G^\mp} \lambda_{AAG^\pm G^\mp} B_0[q^2; G^\pm, G^\pm] + 4\lambda_{Hhh} \lambda_{hAA} B_0[q^2; h, h] + 4\lambda_{HHh} \lambda_{hAA} B_0[q^2; h, H] \\
& + 12\lambda_{HHH} \lambda_{HAA} B_0[q^2; H, H] + 24\lambda_{HAA} \lambda_{AAA} B_0[q^2; A, A] + 6\lambda_{HAG} \lambda_{AAAG} B_0[q^2; A, G] \\
& + 4\lambda_{HGG} \lambda_{AAG} B_0[q^2; G, G] + \lambda_{hAG} \lambda_{hAG} \{B_0[p_1^2; G, h] + B_0[p_2^2; G, h]\} \\
& + 4\lambda_{hAA} \lambda_{hAA} \{B_0[p_1^2; A, h] + B_0[p_2^2; A, h]\} + 2\lambda_{HAG} \lambda_{HHAG} \{B_0[p_1^2; G, H] + B_0[p_2^2; G, H]\} \\
& + 8\lambda_{HAA} \lambda_{HAA} \{B_0[p_1^2; H, A] + B_0[p_2^2; H, A]\} \\
& - 2\lambda_{HH+H-} |\lambda_{AH^\pm G^\mp}|^2 C_0[H^\pm, G^\pm, H^\pm] - 2\lambda_{HG+G-} |\lambda_{AH^\pm G^\mp}|^2 C_0[G^\pm, H^\pm, G^\pm] \\
& - 8\lambda_{Hhh} \lambda_{hAA}^2 C_0[h, A, h] - 2\lambda_{Hhh} \lambda_{hGA}^2 C_0[h, G, h] - 8\lambda_{hHH} \lambda_{hAA}^2 C_0[h, A, H] \\
& - 2\lambda_{hHH} \lambda_{hGA} \lambda_{HG} C_0[h, G, H] - 8\lambda_{hHH} \lambda_{hAA}^2 C_0[H, A, h] - 2\lambda_{hHH} \lambda_{hGA} \lambda_{HG} C_0[H, G, h] \\
& - 24\lambda_{HHH} \lambda_{HAA}^2 C_0[H, A, H] - 6\lambda_{HHH} \lambda_{HG}^2 C_0[H, G, H] - 8\lambda_{HAA} \lambda_{hAA}^2 C_0[A, h, A] \\
& - 8\lambda_{HAA}^3 C_0[A, H, A] - 2\lambda_{HGA} \lambda_{hGA} \lambda_{hAA} \{C_0[G, h, A] + C_0[A, h, G]\} \\
& - 2\lambda_{HGA}^2 \lambda_{HAA} \{C_0[G, H, A] + C_0[A, H, G]\} - 2\lambda_{HGG} \lambda_{hGA}^2 C_0[G, h, G] - 2\lambda_{HGG} \lambda_{HG}^2 C_0[G, H, G], \tag{B9}
\end{aligned}$$

$$\begin{aligned}
& (16\pi^2) \Gamma_{HH^+H^-,B}^{\text{IPI}}[p_1^2, p_2^2, q^2] = \\
& \frac{g^4}{4} v c_{\beta-\alpha} (4B_0[q^2; W, W] - 2) + \frac{g_Z^4}{8} c_{2W}^2 v c_{\beta-\alpha} (4B_0[q^2; Z, Z] - 2) \\
& - \frac{g^4}{8} v c_{\beta-\alpha}^3 C_{VSV}^{\phi\phi\phi}[W, h, W] - \frac{g^4}{8} v s_{\beta-\alpha}^2 c_{\beta-\alpha} C_{VSV}^{\phi\phi\phi}[W, H, W] - \frac{g^4}{8} v c_{\beta-\alpha} C_{VSV}^{\phi\phi\phi}[W, A, W] \\
& - \frac{g_Z^4}{8} v c_{2W}^2 c_{\beta-\alpha} C_{VSV}^{\phi\phi\phi}[Z, H^+, Z] + \frac{g^2}{4} s_{\beta-\alpha} c_{\beta-\alpha} \lambda_{hH^+H^-} C_{VSS}^{\phi\phi\phi}[W, h, H^-] \\
& - \frac{g^2}{4} s_{\beta-\alpha}^2 \lambda_{HH^+H^-} C_{VSS}^{\phi\phi\phi}[W, H, H^-] - \frac{g^2}{4} c_{\beta-\alpha}^2 \lambda_{hG^+H^-} C_{VSS}^{\phi\phi\phi}[W, h, G^-] \\
& + \frac{g^2}{4} s_{\beta-\alpha} c_{\beta-\alpha} \lambda_{HG^+H^-} C_{VSS}^{\phi\phi\phi}[W, H, G^-] - \frac{g^2}{4} c_{\beta-\alpha} \frac{m_{H^+}^2 - m_A^2}{v} C_{VSS}^{\phi\phi\phi}[W, A, G^-] \\
& + \frac{g^2}{2} c_{\beta-\alpha}^2 \lambda_{hhH} C_{SVS}^{\phi\phi\phi}[h, W, h] - \frac{g^2}{2} s_{\beta-\alpha} c_{\beta-\alpha} \lambda_{hHH} \{C_{SVS}^{\phi\phi\phi}[h, W, H] + C_{SVS}^{\phi\phi\phi}[H, W, h]\} \\
& + \frac{3g^2}{2} s_{\beta-\alpha}^2 \lambda_{HHH} C_{SVS}^{\phi\phi\phi}[H, W, H] + \frac{g^2}{2} \lambda_{HAA} C_{SVS}^{\phi\phi\phi}[A, W, A] + \frac{g_Z^2}{4} c_{2W}^2 \lambda_{HH^+H^-} C_{SVS}^{\phi\phi\phi}[H^-, Z, H^-] \\
& + e^2 \lambda_{HH^+H^-} C_{SVS}^{\phi\phi\phi}[H^-, \gamma, H^-] + \frac{g^2}{4} s_{\beta-\alpha} c_{\beta-\alpha} \lambda_{hH^+H^-} C_{SSV}^{\phi\phi\phi}[H^-, h, W] \\
& - \frac{g^2}{4} s_{\beta-\alpha}^2 \lambda_{HH^+H^-} C_{SSV}^{\phi\phi\phi}[H^-, H, W] - \frac{g^2}{4} c_{\beta-\alpha}^2 \lambda_{hH^+G^-} C_{SSV}^{\phi\phi\phi}[G^-, h, W] \\
& + \frac{g^2}{4} s_{\beta-\alpha} c_{\beta-\alpha} \lambda_{HH^+G^-} C_{SSV}^{\phi\phi\phi}[G^-, H, W] - \frac{g^2}{4} c_{\beta-\alpha} \frac{m_{H^+}^2 - m_A^2}{v} C_{SSV}^{\phi\phi\phi}[G^-, A, W] \\
& + 4\lambda_{HH^+H^-} \lambda_{H^+H^-H^+H^-} B_0[q^2; H^+, H^+] + \lambda_{HG^+G^-} \lambda_{H^+H^-G^+G^-} B_0[q^2; G^+, G^+] \\
& + 4\lambda_{HH^+G^-} \lambda_{H^+H^-H^+G^-} B_0[q^2; H^+, G^+] + \lambda_{hH^+H^-} \lambda_{hH^+H^-} (B_0[p_1^2; H^+, h] + B_0[p_2^2; H^+, h]) \\
& + 2\lambda_{HH^+H^-} \lambda_{HHH^+H^-} (B_0[p_1^2; H^+, H] + B_0[p_2^2; H^+, H]) \\
& + 2\lambda_{HH^+G^-} \lambda_{HHG^+H^-} B_0[p_1^2; G^-, H] + 2\lambda_{HG^+H^-} \lambda_{HHH^+G^-} B_0[p_2^2; G^+, H] \\
& + \lambda_{hH^+G^-} \lambda_{hH^+G^-} B_0[p_1^2; G^-, h] + \lambda_{hG^+H^-} \lambda_{hH^+G^-} B_0[p_2^2; G^+, h] \\
& + \lambda_{AH^+G^-} \lambda_{HAG^+H^-} B_0[p_1^2; G^-, A] + \lambda_{AG^+H^-} \lambda_{HAH^+G^-} B_0[p_2^2; G^+, A] \\
& + 2\lambda_{hhH} \lambda_{hhH^+H^-} B_0[q^2; h, h] + 2\lambda_{hHH} \lambda_{hH^+H^-} B_0[q^2; h, H] + 6\lambda_{HHH} \lambda_{HHH^+H^-} B_0[q^2; H, H] \\
& + 2\lambda_{HAA} \lambda_{AAH^+H^-} B_0[q^2; A, A] + \lambda_{HAG} \lambda_{GAH^+H^-} B_0[q^2; A, G^0] + 2\lambda_{HGG} \lambda_{GGH^+H^-} B_0[q^2; G^0, G^0] \\
& - \lambda_{HH^+H^-} (\lambda_{hH^+H^-}^2 C_0[H^-, h, H^-] + \lambda_{HH^+H^-}^2 C_0[H^-, H, H^-]) \\
& - 2\lambda_{hhH} \lambda_{hH^+H^-}^2 C_0[h, H^+, h] - 6\lambda_{HHH} \lambda_{HH^+H^-}^2 C_0[H, H^+, H] \\
& - 2\lambda_{hHH} \lambda_{hH^+H^-} \lambda_{HH^+H^-} (C_0[h, H^+, H] + C_0[H, H^+, h]) \\
& - \lambda_{HH^+G^-} (\lambda_{hH^+H^-} \lambda_{hG^+H^-} C_0[H^-, h, G^-] + \lambda_{HH^+H^-} \lambda_{HG^+H^-} C_0[H^-, H, G^-]) \\
& - \lambda_{HG^+H^-} (\lambda_{hH^+H^-} \lambda_{hH^+G^-} C_0[G^-, h, H^-] + \lambda_{HH^+H^-} \lambda_{HH^+G^-} C_0[G^-, H, H^-]) \\
& - 2\lambda_{hhH} \lambda_{hH^+G^-}^2 C_0[h, G^+, h] - 6\lambda_{HHH} \lambda_{HH^+G^-}^2 C_0[H, G^+, H]
\end{aligned}$$

$$\begin{aligned}
& -2\lambda_{hHH}\lambda_{hH+G^-}\lambda_{HH+G^-}(C_0[h, G^+, H] + C_0[H, G^+, h]) \\
& -2\lambda_{HAA}|\lambda_{AH+G^-}|^2C_0[A, G^+, A] - \lambda_{HG+G^-}(\lambda_{hH+G^-}^2C_0[G^-, h, G^-] + \lambda_{HH+G^-}^2C_0[G^-, H, G^-]) \\
& - \lambda_{HG+G^-}|\lambda_{AH+G^-}|^2C_0[G^-, A, G^-], \tag{B10}
\end{aligned}$$

where the definition of the coupling factor κ_f^H is given in Ref. [21]. B_i and C_i functions represent Passarino-Veltman functions [108] with

$$B_i[p_j^2; X, Y] \equiv B_i[p_j^2; m_X, m_Y], \tag{B11}$$

$$C_i[X, Y, Z] \equiv C_i[p_1^2, p_2^2, q^2; m_X, m_Y, m_Z]. \tag{B12}$$

Each combination of C -functions is defined as,

$$\begin{aligned}
C_{SVV}^{\phi\phi\phi}[S, V_1, V_2] &= [p_1^2C_{21} + p_2^2C_{22} + 2p_1 \cdot p_2C_{23} + 4C_{24} - \frac{1}{2} \\
&\quad - (q + p_1) \cdot (p_1C_{11} + p_2C_{12}) + q \cdot p_1C_0](S, V_1, V_2), \tag{B13}
\end{aligned}$$

$$\begin{aligned}
C_{VSV}^{\phi\phi\phi}[V_2, S, V_1] &= [p_1^2C_{21} + p_2^2C_{22} + 2p_1 \cdot p_2C_{23} + 4C_{24} - \frac{1}{2} \\
&\quad + (3p_1 - p_2) \cdot (p_1C_{11} + p_2C_{12}) + 2p_1 \cdot (p_1 - p_2)C_0](V_2, S, V_1), \tag{B14}
\end{aligned}$$

$$\begin{aligned}
C_{VVS}^{\phi\phi\phi}[V_1, V_2, S] &= [p_1^2C_{21} + p_2^2C_{22} + 2p_1 \cdot p_2C_{23} + 4C_{24} - \frac{1}{2} \\
&\quad + (3p_1 + 4p_2) \cdot (p_1C_{11} + p_2C_{12}) + 2q \cdot (q + p_2)C_0](V_1, V_2, S), \tag{B15}
\end{aligned}$$

$$\begin{aligned}
C_{VSS}^{\phi\phi\phi}[V, S_1, S_2] &= [p_1^2C_{21} + p_2^2C_{22} + 2p_1 \cdot p_2C_{23} + 4C_{24} - \frac{1}{2} \\
&\quad + (4p_1 + 2p_2) \cdot (p_1C_{11} + p_2C_{12}) + 4q \cdot p_1C_0](V, S_1, S_2), \tag{B16}
\end{aligned}$$

$$\begin{aligned}
C_{SVS}^{\phi\phi\phi}[S_2, V, S_1] &= [p_1^2C_{21} + p_2^2C_{22} + 2p_1 \cdot p_2C_{23} + 4C_{24} - \frac{1}{2} \\
&\quad + 2p_2 \cdot (p_1C_{11} + p_2C_{12}) - p_1 \cdot (p_1 + 2p_2)C_0](S_2, V, S_1), \tag{B17}
\end{aligned}$$

$$\begin{aligned}
C_{SSV}^{\phi\phi\phi}[S_1, S_2, V] &= [p_1^2C_{21} + p_2^2C_{22} + 2p_1 \cdot p_2C_{23} + 4C_{24} - \frac{1}{2} \\
&\quad - 2p_2 \cdot (p_1C_{11} + p_2C_{12}) - q \cdot (p_1 - p_2)C_0](S_1, S_2, V). \tag{B18}
\end{aligned}$$

The first two Eqs. (B7) and (B8) and the latter two Eq. (B9) and (B10) are fermion loop contributions and boson loop contributions, respectively. The definition of momentum is given in Sec. III.

As mentioned in Sec. III, the non-vanishing contribution from mixing self-energies is included in the electroweak corrections to the decay rate $H \rightarrow H^+H^-$, which is calculated as,

$$\Delta_{\text{mix}}(H \rightarrow H^+H^-) = -4 \frac{\lambda_{HH+G^-} \hat{\Pi}_{H+G^-}(m_{H^\pm}^2)}{\lambda_{HH+H^-} m_{H^\pm}^2}. \quad (\text{B19})$$

2. hHH, hAA, hH^+H^- vertices in the IDM

We here give explicit formulae for counterterms and 1PI diagram contributions of the hHH, hAA, hH^+H^- vertices in the IDM.

The explicit formula of the counterterm of the $h\phi\phi$ ($\phi = H, A, H^\pm$) is given by

$$\delta\Gamma_{h\phi\phi} = 2\delta\lambda_{h\phi\phi} + C_\phi \lambda_{h\phi\phi} \left(\delta Z_\phi + \frac{1}{2} \delta Z_h \right), \quad (\text{B20})$$

with

$$\delta\lambda_{h\phi\phi} = -\frac{1}{v} \delta m_\phi^2 + \frac{m_\phi^2 - \mu_2^2}{v^2} \delta v + \frac{1}{v} \delta \mu_2^2, \quad (\text{B21})$$

$$C_H = C_A = 2, \quad C_{H^\pm} = 1. \quad (\text{B22})$$

$\delta\mu_2^2$ is determined by $\overline{\text{MS}}$ scheme as well as δM^2 in the THDM, so that it is given by

$$\delta\mu_2^2 = \frac{1}{16\pi^2} \left[-\frac{m_h^2}{2v^2} (m_H^2 + m_A^2 + 2m_{H^\pm}^2) + \frac{\mu_2^2}{v^2} (2m_h^2 - 6m_W^2 - 3m_Z^2 + 3\lambda_2 v^2) \right] \Delta_{\text{div}}. \quad (\text{B23})$$

The 1PI diagram contributions to the $h\Phi\Phi$ vertex are calculated as

$$\begin{aligned} & (16\pi^2) \Gamma_{hHH,B}^{\text{1PI}}[q^2, p_1^2, p_2^2] = \\ & 12\lambda_{hhh} \lambda_{hHH} B_0[q^2; h, h] + 24\lambda_{hHH} \lambda_{HHHH} B_0[q^2; H, H] + 4\lambda_{hAA} \lambda_{HHA} B_0[q^2; A, A] \\ & + 4\lambda_{hGG} \lambda_{HHGG} B_0[q^2; G^0, G^0] + 2\lambda_{hH^+H^-} \lambda_{HHH^+H^-} B_0[q^2; H^\pm, H^\pm] + 2\lambda_{hG^+G^-} \lambda_{HHG^+G^-} B_0[q^2; G^\pm, G^\pm] \\ & + 8\lambda_{hHH} \lambda_{hHH} (B_0[p_1^2; h, H] + B_0[p_2^2; h, H]) + \lambda_{HAG} \lambda_{hHAG} (B_0[p_1^2; G^0, A] + B_0[p_2^2; G^0, A]) \\ & + 2\lambda_{HH+G^-} \lambda_{hHH-G^+} (B_0[p_1^2; G^\pm, H^\pm] + B_0[p_2^2; G^\pm, H^\pm]) \\ & + 2g^3 m_W (B_0[q^2; W, W] - \frac{1}{2}) + g_Z^3 m_Z (B_0[q^2; Z, Z] - \frac{1}{2}) \\ & - \frac{g_Z^4}{8} v C_{VSV}^{\phi\phi\phi} [Z, A, Z] - \frac{g^4}{4} v C_{VSV}^{\phi\phi\phi} [W, H^\pm, W] + \frac{g_Z^2}{2} \lambda_{hAA} C_{SVS}^{\phi\phi\phi} [A, Z, A] + \frac{g^2}{2} \lambda_{hH^+H^-} C_{SVS}^{\phi\phi\phi} [H^\pm, W, H^\pm] \\ & + \frac{g_Z^2}{4} \lambda_{HAG} (C_{VSS}^{\phi\phi\phi} [Z, A, G^0] + C_{SSV}^{\phi\phi\phi} [G^0, A, Z]) + \frac{g^2}{2} \lambda_{HH+G^-} (C_{VSS}^{\phi\phi\phi} [W, H^\pm, G^\pm] + C_{SSV}^{\phi\phi\phi} [G^\pm, H^\pm, W]) \\ & - 24\lambda_{hhh} \lambda_{hHH}^2 C_0[h, H, h] - 8\lambda_{hHH}^3 C_0[H, h, H] - 2\lambda_{hAA} \lambda_{HAG}^2 C_0[A, G^0, A] - 2\lambda_{hGG} \lambda_{HAG}^2 C_0[G^0, A, G^0] \\ & - 2\lambda_{hH^+H^-} |\lambda_{HH+G^-}|^2 C_0[H^\pm, G^\pm, H^\pm] - 2\lambda_{hG^+G^-} |\lambda_{HH+G^-}|^2 C_0[G^\pm, H^\pm, G^\pm], \quad (\text{B24}) \end{aligned}$$

$$\begin{aligned}
& (16\pi^2)\Gamma_{hAA}^{\text{1PI,B}}[q^2, p_1^2, p_2^2] = \\
& 24\lambda_{hAA}\lambda_{AAAA}B_0[q^2; A, A] + 8\lambda_{hAA}\lambda_{hhAA}(B_0[p_1^2; h, A] + B_0[p_2^2; h, A]) + 4\lambda_{hHH}\lambda_{HHAA}B_0[q^2; H, H] \\
& + 12\lambda_{hhh}\lambda_{hhAA}B_0[q^2; h, h] + 4\lambda_{hGG}\lambda_{AAGG}B_0[q^2; G^0, G^0] + \lambda_{HAG}\lambda_{hHAG}(B_0[p_1^2; H, G^0] + B_0[p_2^2; H, G^0]) \\
& + 2\lambda_{hG+G-}\lambda_{AAG+G-}B_0[q^2; G^\pm, G^\pm] + 2\lambda_{AH-G+}\lambda_{hAH+G-}(B_0[p_1^2; H^\pm, G^\pm] + B_0[p_2^2; H^\pm, G^\pm]) \\
& + 2\lambda_{hH+H-}\lambda_{AAH+H-}B_0[q^2; H^\pm, H^\pm] \\
& + 2g^3m_W(B_0[q^2; W, W] - \frac{1}{2}) + g_Z^3m_Z(B_0[q^2; Z, Z] - \frac{1}{2}) \\
& - \frac{g_Z^4}{8}vC_{VSV}^{\phi\phi\phi}[Z, H, Z] - \frac{g^4}{4}vC_{VSV}^{\phi\phi\phi}[W, H^\pm, W] + \frac{g_Z^2}{2}\lambda_{hHH}C_{SVS}^{\phi\phi\phi}[H, Z, H] + \frac{g^2}{2}\lambda_{hH+H-}C_{SVS}^{\phi\phi\phi}[H^\pm, W, H^\pm] \\
& + i\frac{g^2}{2}\lambda_{AH+G-}(C_{VSS}^{\phi\phi\phi}[W, H^\pm, G^\pm] + C_{SSV}^{\phi\phi\phi}[G^\pm, H^\pm, W]) - \frac{g_Z^2}{4}\lambda_{HAG}(C_{VSS}^{\phi\phi\phi}[Z, H, G^0] + C_{SSV}^{\phi\phi\phi}[G^0, H, Z]) \\
& - 24\lambda_{hhh}\lambda_{hAA}^2C_0[h, A, h] - 2\lambda_{hHH}\lambda_{HAG}^2C_0[H, G^0, H] - 8\lambda_{hAA}^3C_0[A, h, A] \\
& - 2\lambda_{hGG}\lambda_{HAG}^2C_0[G^0, H, G^0] - 2\lambda_{hH+H-}\lambda_{AH+G-}\lambda_{AH-G+}C_0[H^\pm, G^\pm, H^\pm] \\
& - 2\lambda_{hG+G-}\lambda_{AH+G-}\lambda_{AH-G+}C_0[G^\pm, H^\pm, G^\pm], \tag{B25}
\end{aligned}$$

$$\begin{aligned}
& (16\pi^2)\Gamma_{hH+H-}^{\text{1PI,B}}[q^2, p_1^2, p_2^2] \\
& = 6\lambda_{hhh}\lambda_{hhH+H-}B_0[q^2; h, h] + 2\lambda_{hH+H-}\lambda_{hhH+H-}(B_0[p_1^2; h, H^\pm] + B_0[p_2^2; h, H^\pm]) \\
& + 2\lambda_{hHH}\lambda_{HHH+H-}B_0[q^2; H, H] + \lambda_{HG+H-}\lambda_{hHH+G-}(B_0[p_1^2; H, G^\pm] + B_0[p_2^2; H, G^\pm]) \\
& + 2\lambda_{hAA}\lambda_{AAH+H-}B_0[q^2; A, A] + \lambda_{AG+H-}\lambda_{hAH+G-}(B_0[p_1^2; A, G^\pm] + B_0[p_2^2; A, G^\pm]) \\
& + 2\lambda_{hG^0G^0}\lambda_{G^0G^0H+H-}B_0[q^2; G^0, G^0] + 4\lambda_{hH+H-}\lambda_{H+H-H+H-}B_0[q^2; H^\pm, H^\pm]) \\
& + \lambda_{hG+G-}\lambda_{H+H-G+G-}B_0[q^2; G^\pm, G^\pm]) \\
& + 2g^3m_W(B_0[q^2; W, W] - \frac{1}{2}) + c_{2W}^2g_Z^3m_Z(B_0[q^2; Z, Z] - \frac{1}{2}) \\
& - \frac{g^4v}{8}C_{VSV}^{\phi\phi\phi}[W, H, W] - \frac{g^4v}{8}C_{VSV}^{\phi\phi\phi}[W, A, W] - \frac{g_Z^4v}{8}c_{2W}^2C_{VSV}^{\phi\phi\phi}[Z, H^+, Z] \\
& + \frac{g^2}{2}\lambda_{hHH}C_{SVS}^{\phi\phi\phi}[H, W, H] + \frac{g^2}{2}\lambda_{hAA}C_{SVS}^{\phi\phi\phi}[A, W, A] + \frac{g_Z^2}{4}c_{2W}^2\lambda_{hH+H-}C_{SVS}^{\phi\phi\phi}[H^+, Z, H^+] \\
& + e^2\lambda_{hH+H-}C_{VSV}^{\phi\phi\phi}[H^+, \gamma, H^+] - \frac{g^2}{4}\lambda_{HH-G+}(C_{VSS}^{\phi\phi\phi}[W, H, G^+] + C_{SSV}^{\phi\phi\phi}[G^+, H, W]) \\
& + i\frac{g^2}{4}\lambda_{AH-G+}(C_{VSS}^{\phi\phi\phi}[W, A, G^+] + C_{SSV}^{\phi\phi\phi}[G^+, A, W]) \\
& - 6\lambda_{hhh}\lambda_{hH+H-}^2C_0[h, H^+, h] - 2\lambda_{hHH}\lambda_{HH+G-}\lambda_{HH-G+}C_0[H, G^+, H] \\
& - 2\lambda_{hAA}\lambda_{AH+G-}\lambda_{AH-G+}C_0[A, G^+, A] - \lambda_{hH+H-}^3C_0[H^+, h, H^+] \\
& - \lambda_{hG+G-}\lambda_{HH+G-}\lambda_{HH-G+}C_0[G^+, H, G^+] - \lambda_{hG+G-}\lambda_{AH+G-}\lambda_{AH-G+}C_0[G^+, H, H^+]. \tag{B26}
\end{aligned}$$

Appendix C: $\phi \rightarrow H^+ H^- \gamma$

We here give the explicit formula of the real photon emission process for $\phi \rightarrow H^+ H^-$, which cancels IR divergence of the virtual corrections for the $\phi H^+ H^-$ vertex. The formula of the decay rate can be expressed as

$$\Gamma[\phi \rightarrow H^+ H^- \gamma] = \frac{e^2 \lambda_{\phi H^+ H^-}^2}{16\pi^3 m_\phi} \{ -I_1 - I_2 - m_{H^\pm}^2 I_{11} - m_{H^\pm}^2 I_{22} - (2m_{H^\pm}^2 - m_\phi^2) I_{12} \}, \quad (\text{C1})$$

where definitions of I -functions are given in Appendix D of Ref. [25].

-
- [1] G. Aad *et al.* (ATLAS), *Nature* **607**, 52 (2022), [Erratum: *Nature* 612, E24 (2022)], arXiv:2207.00092 [hep-ex].
 - [2] A. Tumasyan *et al.* (CMS), *Nature* **607**, 60 (2022), arXiv:2207.00043 [hep-ex].
 - [3] G. Apollinari, I. Béjar Alonso, O. Brüning, P. Fessia, M. Lamont, L. Rossi, and L. Tavian, 10.23731/CYRM-2017-004.
 - [4] H. Baer, T. Barklow, K. Fujii, Y. Gao, A. Hoang, S. Kanemura, J. List, H. E. Logan, A. Nomerotski, M. Perelstein, *et al.*, (2013), arXiv:1306.6352 [hep-ph].
 - [5] K. Fujii *et al.*, (2017), arXiv:1710.07621 [hep-ex].
 - [6] S. Asai, J. Tanaka, Y. Ushiroda, M. Nakao, J. Tian, S. Kanemura, S. Matsumoto, S. Shirai, M. Endo, and M. Kakizaki, (2017), arXiv:1710.08639 [hep-ex].
 - [7] K. Fujii *et al.* (LCC Physics Working Group), (2019), arXiv:1908.11299 [hep-ex].
 - [8] CEPC-SPPC Study Group, CEPC-SPPC Preliminary Conceptual Design Report. 1. Physics and Detector.
 - [9] M. Bicer *et al.* (TLEP Design Study Working Group), *Proceedings, 2013 Community Summer Study on the Future of U.S. Particle Physics: Snowmass on the Mississippi (CSS2013): Minneapolis, MN, USA, July 29-August 6, 2013*, *JHEP* **01**, 164 (2014), arXiv:1308.6176 [hep-ex].
 - [10] J. de Blas *et al.*, *JHEP* **01**, 139 (2020), arXiv:1905.03764 [hep-ph].
 - [11] S. Kanemura and R. Nagai, *JHEP* **03**, 194 (2022), arXiv:2111.12585 [hep-ph].
 - [12] M. Aiko, S. Kanemura, M. Kikuchi, K. Mawatari, K. Sakurai, and K. Yagyu, *Nucl. Phys. B* **966**, 115375 (2021), arXiv:2010.15057 [hep-ph].
 - [13] K. Cheung, A. Jueid, J. Kim, S. Lee, C.-T. Lu, and J. Song, *Phys. Rev. D* **105**, 095044 (2022), arXiv:2201.06890 [hep-ph].
 - [14] A. Arhrib, R. Benbrik, and S. Moretti, *Eur. Phys. J. C* **77**, 621 (2017), arXiv:1607.02402 [hep-ph].
 - [15] S. Kanemura, S. Kiyoura, Y. Okada, E. Senaha, and C. P. Yuan, *Phys. Lett.* **B558**, 157 (2003), arXiv:hep-ph/0211308 [hep-ph].

- [16] S. Kanemura, Y. Okada, and E. Senaha, Phys. Lett. **B606**, 361 (2005), arXiv:hep-ph/0411354 [hep-ph].
- [17] S. Kanemura, Y. Okada, E. Senaha, and C. P. Yuan, Phys. Rev. **D70**, 115002 (2004), arXiv:hep-ph/0408364 [hep-ph].
- [18] S. Kanemura, M. Kikuchi, K. Sakurai, and K. Yagyu, Comput. Phys. Commun. **233**, 134 (2018), arXiv:1710.04603 [hep-ph].
- [19] S. Kanemura, M. Kikuchi, K. Mawatari, K. Sakurai, and K. Yagyu, Comput. Phys. Commun. **257**, 107512 (2020), arXiv:1910.12769 [hep-ph].
- [20] S. Kanemura, M. Kikuchi, K. Sakurai, and K. Yagyu, Phys. Rev. **D96**, 035014 (2017), arXiv:1705.05399 [hep-ph].
- [21] S. Kanemura, M. Kikuchi, and K. Yagyu, Nucl. Phys. B **983**, 115906 (2022), arXiv:2203.08337 [hep-ph].
- [22] M. Aiko, S. Kanemura, and K. Sakurai, Nucl. Phys. B **986**, 116047 (2023), arXiv:2207.01032 [hep-ph].
- [23] M. Aiko, S. Kanemura, and K. Sakurai, Nucl. Phys. B **973**, 115581 (2021), arXiv:2108.11868 [hep-ph].
- [24] W. F. L. Hollik, Fortsch. Phys. **38**, 165 (1990).
- [25] A. Denner, Fortsch. Phys. **41**, 307 (1993), arXiv:0709.1075 [hep-ph].
- [26] J. Fleischer and F. Jegerlehner, Phys. Rev. **D23**, 2001 (1981).
- [27] T. N. Dao, L. Fritz, M. Krause, M. Mühlleitner, and S. Patel, Eur. Phys. J. C **80**, 292 (2020), arXiv:1911.07197 [hep-ph].
- [28] M. Krause and M. Mühlleitner, JHEP **04**, 083 (2020), arXiv:1912.03948 [hep-ph].
- [29] S. M. Oliveira, L. Brucher, R. Santos, and A. Barroso, Phys. Rev. D **64**, 017301 (2001), arXiv:hep-ph/0011324.
- [30] A. G. Akeroyd, A. Arhrib, and E.-M. Naimi, Eur. Phys. J. C **12**, 451 (2000), [Erratum: Eur.Phys.J.C 14, 371 (2000)], arXiv:hep-ph/9811431.
- [31] A. G. Akeroyd, A. Arhrib, and E. Naimi, Eur. Phys. J. C **20**, 51 (2001), arXiv:hep-ph/0002288.
- [32] M. Krause, R. Lorenz, M. Muhlleitner, R. Santos, and H. Ziesche, JHEP **09**, 143 (2016), arXiv:1605.04853 [hep-ph].
- [33] M. Krause, M. Muhlleitner, R. Santos, and H. Ziesche, Phys. Rev. D **95**, 075019 (2017), arXiv:1609.04185 [hep-ph].
- [34] R. Santos, A. Barroso, and L. Brucher, Phys. Lett. B **391**, 429 (1997), arXiv:hep-ph/9608376.
- [35] V. D. Barger, M. S. Berger, A. L. Stange, and R. J. N. Phillips, Phys. Rev. D **45**, 4128 (1992).
- [36] P. H. Chankowski, S. Pokorski, and J. Rosiek, Nucl. Phys. B **423**, 497 (1994).
- [37] P. Osland and P. N. Pandita, Phys. Rev. D **59**, 055013 (1999), arXiv:hep-ph/9806351.
- [38] Y. P. Philippov, Phys. Atom. Nucl. **70**, 1288 (2007), arXiv:hep-ph/0611260.
- [39] K. E. Williams, H. Rzehak, and G. Weiglein, Eur. Phys. J. C **71**, 1669 (2011), arXiv:1103.1335 [hep-ph].
- [40] K. E. Williams and G. Weiglein, Phys. Lett. B **660**, 217 (2008), arXiv:0710.5320 [hep-ph].

- [41] M. Krause, M. Mühlleitner, and M. Spira, *Comput. Phys. Commun.* **246**, 106852 (2020), arXiv:1810.00768 [hep-ph].
- [42] A. Denner, S. Dittmaier, and A. Mück, *Comput. Phys. Commun.* **254**, 107336 (2020), arXiv:1912.02010 [hep-ph].
- [43] M. Krause and M. Mühlleitner, (2019), 10.1016/j.cpc.2019.106924, arXiv:1904.02103 [hep-ph].
- [44] F. Egle, M. Mühlleitner, R. Santos, and J. a. Viana, (2023), arXiv:2306.04127 [hep-ph].
- [45] P. Athron, A. Büchner, D. Harries, W. Kotlarski, D. Stöckinger, and A. Voigt, *Comput. Phys. Commun.* **283**, 108584 (2023), arXiv:2106.05038 [hep-ph].
- [46] S. Kanemura, M. Kikuchi, and K. Yagyu, *Nucl. Phys.* **B907**, 286 (2016), arXiv:1511.06211 [hep-ph].
- [47] S. Kanemura, M. Kikuchi, and K. Yagyu, *Nucl. Phys.* **B917**, 154 (2017), arXiv:1608.01582 [hep-ph].
- [48] G. M. Pruna and T. Robens, *Phys. Rev.* **D88**, 115012 (2013), arXiv:1303.1150 [hep-ph].
- [49] K. Fuyuto and E. Senaha, *Phys. Rev. D* **90**, 015015 (2014), arXiv:1406.0433 [hep-ph].
- [50] T. Robens and T. Stefaniak, *Eur. Phys. J.* **C75**, 104 (2015), arXiv:1501.02234 [hep-ph].
- [51] G. Cynolter, E. Lendvai, and G. Pocsik, *Acta Phys. Polon.* **B36**, 827 (2005), arXiv:hep-ph/0410102 [hep-ph].
- [52] C.-Y. Chen, S. Dawson, and I. M. Lewis, *Phys. Rev.* **D91**, 035015 (2015), arXiv:1410.5488 [hep-ph].
- [53] M. Gonderinger, Y. Li, H. Patel, and M. J. Ramsey-Musolf, *JHEP* **01**, 053 (2010), arXiv:0910.3167 [hep-ph].
- [54] D. Lopez-Val and T. Robens, *Phys. Rev.* **D90**, 114018 (2014), arXiv:1406.1043 [hep-ph].
- [55] S. Kanemura, M. Kikuchi, and K. Yagyu, *Phys. Lett.* **B731**, 27 (2014), arXiv:1401.0515 [hep-ph].
- [56] S. Kanemura, M. Kikuchi, and K. Yagyu, *Nucl. Phys.* **B896**, 80 (2015), arXiv:1502.07716 [hep-ph].
- [57] N. G. Deshpande and E. Ma, *Phys. Rev.* **D18**, 2574 (1978).
- [58] K. G. Klimenko, *Theor. Math. Phys.* **62**, 58 (1985).
- [59] M. Sher, *Phys. Rept.* **179**, 273 (1989).
- [60] S. Nie and M. Sher, *Phys. Lett.* **B449**, 89 (1999), arXiv:hep-ph/9811234 [hep-ph].
- [61] S. Kanemura, T. Kasai, and Y. Okada, *Phys. Lett.* **B471**, 182 (1999), arXiv:hep-ph/9903289 [hep-ph].
- [62] S. Kanemura, T. Kubota, and E. Takasugi, *Phys. Lett.* **B313**, 155 (1993), arXiv:hep-ph/9303263 [hep-ph].
- [63] A. G. Akeroyd, A. Arhrib, and E.-M. Naimi, *Phys. Lett.* **B490**, 119 (2000), arXiv:hep-ph/0006035 [hep-ph].
- [64] I. F. Ginzburg and I. P. Ivanov, *Phys. Rev.* **D72**, 115010 (2005), arXiv:hep-ph/0508020 [hep-ph].
- [65] S. Kanemura and K. Yagyu, *Phys. Lett.* **B751**, 289 (2015), arXiv:1509.06060 [hep-ph].
- [66] V. Branchina, F. Contino, and P. M. Ferreira, *JHEP* **11**, 107 (2018), arXiv:1807.10802 [hep-ph].
- [67] K. Inoue, A. Kakuto, H. Komatsu, and S. Takeshita, *Prog. Theor. Phys.* **67**, 1889 (1982).
- [68] D. Toussaint, *Phys. Rev.* **D18**, 1626 (1978).
- [69] S. Bertolini, *Nucl. Phys.* **B272**, 77 (1986).
- [70] M. E. Peskin and J. D. Wells, *Phys. Rev.* **D64**, 093003 (2001), arXiv:hep-ph/0101342 [hep-ph].

- [71] W. Grimus, L. Lavoura, O. M. Ogreid, and P. Osland, Nucl. Phys. **B801**, 81 (2008), arXiv:0802.4353 [hep-ph].
- [72] S. Kanemura, Y. Okada, H. Taniguchi, and K. Tsumura, Phys. Lett. **B704**, 303 (2011), arXiv:1108.3297 [hep-ph].
- [73] S. Kanemura, M. Kikuchi, and K. Sakurai, Phys. Rev. **D94**, 115011 (2016), arXiv:1605.08520 [hep-ph].
- [74] I. F. Ginzburg, K. A. Kanishev, M. Krawczyk, and D. Sokolowska, Phys. Rev. **D82**, 123533 (2010), arXiv:1009.4593 [hep-ph].
- [75] A. Goudelis, B. Herrmann, and O. Stål, JHEP **09**, 106 (2013), arXiv:1303.3010 [hep-ph].
- [76] S. L. Glashow and S. Weinberg, Phys. Rev. **D15**, 1958 (1977).
- [77] V. D. Barger, J. L. Hewett, and R. J. N. Phillips, Phys. Rev. **D41**, 3421 (1990).
- [78] Y. Grossman, Nucl. Phys. **B426**, 355 (1994), arXiv:hep-ph/9401311 [hep-ph].
- [79] A. G. Akeroyd, Phys. Lett. **B377**, 95 (1996), arXiv:hep-ph/9603445 [hep-ph].
- [80] M. Aoki, S. Kanemura, K. Tsumura, and K. Yagyu, Phys. Rev. **D80**, 015017 (2009), arXiv:0902.4665 [hep-ph].
- [81] R. Barbieri, L. J. Hall, and V. S. Rychkov, Phys. Rev. **D74**, 015007 (2006), arXiv:hep-ph/0603188 [hep-ph].
- [82] B. W. Lee, C. Quigg, and H. B. Thacker, Phys. Rev. **D16**, 1519 (1977).
- [83] J. R. Espinosa, T. Konstandin, and F. Riva, Nucl. Phys. **B854**, 592 (2012), arXiv:1107.5441 [hep-ph].
- [84] M. E. Peskin and T. Takeuchi, Phys. Rev. Lett. **65**, 964 (1990).
- [85] M. E. Peskin and T. Takeuchi, Phys. Rev. **D46**, 381 (1992).
- [86] Y. Yamada, Phys. Rev. **D64**, 036008 (2001), arXiv:hep-ph/0103046 [hep-ph].
- [87] J. Papavassiliou, Phys. Rev. D **50**, 5958 (1994), arXiv:hep-ph/9406258.
- [88] S. Dittmaier and H. Rzehak, JHEP **05**, 125 (2022), arXiv:2203.07236 [hep-ph].
- [89] S. Dittmaier and H. Rzehak, JHEP **08**, 245 (2022), arXiv:2206.01479 [hep-ph].
- [90] L. Mihaila, B. Schmidt, and M. Steinhauser, Phys. Lett. **B751**, 442 (2015), arXiv:1509.02294 [hep-ph].
- [91] S. G. Gorishnii, A. L. Kataev, S. A. Larin, and L. R. Surguladze, Mod. Phys. Lett. **A5**, 2703 (1990).
- [92] S. G. Gorishnii, A. L. Kataev, S. A. Larin, and L. R. Surguladze, Phys. Rev. **D43**, 1633 (1991).
- [93] K. G. Chetyrkin and A. Kwiatkowski, Nucl. Phys. **B461**, 3 (1996), arXiv:hep-ph/9505358 [hep-ph].
- [94] S. A. Larin, T. van Ritbergen, and J. A. M. Vermaseren, Phys. Lett. B **362**, 134 (1995), arXiv:hep-ph/9506465.
- [95] M. Drees and K.-i. Hikasa, Phys. Rev. **D41**, 1547 (1990).
- [96] A. Djouadi, Phys. Rept. **459**, 1 (2008), arXiv:hep-ph/0503173.
- [97] A. Djouadi and P. Gambino, Phys. Rev. D **51**, 218 (1995), [Erratum: Phys.Rev.D 53, 4111 (1996)], arXiv:hep-ph/9406431.
- [98] A. Djouadi, J. Kalinowski, and M. Spira, Comput. Phys. Commun. **108**, 56 (1998), arXiv:hep-ph/9704448 [hep-ph].
- [99] S. Dawson and R. Kauffman, Phys. Rev. D **49**, 2298 (1994), arXiv:hep-ph/9310281.

- [100] M. Spira, A. Djouadi, D. Graudenz, and P. M. Zerwas, Nucl. Phys. B **453**, 17 (1995), arXiv:hep-ph/9504378.
- [101] R. Harlander and P. Kant, JHEP **12**, 015 (2005), arXiv:hep-ph/0509189.
- [102] K. G. Chetyrkin, B. A. Kniehl, and M. Steinhauser, Phys. Rev. Lett. **79**, 353 (1997), arXiv:hep-ph/9705240 [hep-ph].
- [103] K. G. Chetyrkin, B. A. Kniehl, M. Steinhauser, and W. A. Bardeen, Nucl. Phys. B **535**, 3 (1998), arXiv:hep-ph/9807241.
- [104] D. Albert, W. J. Marciano, D. Wyler, and Z. Parsa, Nucl. Phys. B **166**, 460 (1980).
- [105] T. Hahn and M. Perez-Victoria, Comput. Phys. Commun. **118**, 153 (1999), arXiv:hep-ph/9807565 [hep-ph].
- [106] S. Kanemura, M. Kikuchi, K. Mawatari, K. Sakurai, and K. Yagyu, Nucl. Phys. B **949**, 114791 (2019), arXiv:1906.10070 [hep-ph].
- [107] R. L. Workman *et al.* (Particle Data Group), PTEP **2022**, 083C01 (2022).
- [108] G. Passarino and M. J. G. Veltman, Nucl. Phys. **B160**, 151 (1979).